Elsevier Editorial System(tm) for Deep-Sea Research Part II

Manuscript Draft

Manuscript Number: DSR2-D-15-00047R1

Title: Controls of primary production in two phytoplankton blooms in the Antarctic Circumpolar Current

Article Type: SI: Eddy-Pump

Corresponding Author: Dr. Clara Jule Marie Hoppe,

Corresponding Author's Institution: Alfred Wegener Institute

First Author: Clara Jule Marie Hoppe

Order of Authors: Clara Jule Marie Hoppe; Christine Klaas, Dr.; Sharyn Ossebaar; Mariana A Soppa; Wee Cheah, Dr.; Laglera M Luis; Santos-Echeandia Juan; Björn Rost, Dr.; Dieter A Wolf-Gladrow, Prof. Dr.; Astrid Bracher, Prof. Dr.; Mario Hoppema, Dr.; Volker Strass, Dr.; Scarlett Trimborn, Prof. Dr.

Abstract: The Antarctic Circumpolar Current has a high potential for primary production and carbon sequestration through the biological pump. In the current study, two large-scale blooms observed in 2012 during a cruise with RV Polarstern were investigated with respect to phytoplankton standing stocks, primary productivity and nutrient budgets. While net primary productivity was similar in both blooms, chlorophyll a -specific photosynthesis was more efficient in the bloom closer to the island of South Georgia (39°W, 50°S) compared to the open ocean bloom further east (12°W, 51°S). We did not find evidence for light being the driver of bloom dynamics as chlorophyll standing stocks up to 165 mg m-2 developed despite mixed layers as deep as 90 m. Since the two bloom regions differ in their distance to shelf areas, potential sources of iron vary. Nutrient (nitrate, phosphate, silicate) deficits were similar in both areas despite different bloom ages, but their ratios indicated more pronounced iron limitation at 12°W compared to 39°W. While primarily the supply of iron and not the availability of light seemed to control onset and duration of the blooms, higher grazing pressure could have exerted a stronger control toward the declining phase of the blooms.

Clara J. M. Hoppe
Alfred Wegener Institute -
Helmholtz Center for Polar and Marine Research
Am Handelshafen 12
27570 Bremerhaven, Germany
Phone: +49 471 4831 2096
Email: Clara.Hoppe@awi.de

October 15th, 2015

Dear Evgeny,

we would like to submit the revised version of our manuscript entitled “Controls of primary production in two phytoplankton blooms in the Antarctic Circumpolar Current” for the ‘Eddy Pump’ special issue in *Deep-Sea Research Part II: Topical Studies in Oceanography*.

We are grateful to the reviewers for their helpful comments on our manuscript. We feel that this round of revisions really improved the presentation of our data and helped to streamline our manuscript. For example, we have invited the colleagues in charge of the iron measurements during ‘Eddy Pump’ to contribute to this manuscript. Therefore, we are now able to provide iron data requested by the two referees.

In the response letter, we address all comments by the reviewers and specify what we have done to improve the manuscript with respect to the specific points raised.

We hope that you find our revised manuscript suitable for publication in this special issue.

Please do not hesitate to contact me if you have any further questions.

Also on behalf of all co-authors,
kind regards,
Clara J. M. Hoppe

Response letter to reviewer comments on our manuscript entitled "Controls of primary production in two phytoplankton blooms in the Antarctic Circumpolar Current"

First of all, we would like to thank both reviewers for their helpful and interesting comments on and suggestions for our manuscript, which clearly increased its quality. In the following, our responses to the specific comments are marked by italic fond.

Reviewer #1:

The paper "Controls of primary production in two phytoplankton blooms in the Antarctic Circumpolar Current" by Hoppe and co-authors uses a combination of satellite and field data to compare and contrast two ACC phytoplankton blooms. The paper is well written but a little short on detail. There are results from the study that are not revealed until the discussion section (e.g. iron concentrations, some taxonomy, etc.). I suppose this is because these particular results are in another paper in this special issue, but it makes the present paper more difficult to evaluate. I would suggest putting all of the information required to evaluate these blooms into the results section of this paper, which is fairly short at only 2 double-spaced pages. There are also some issues with the data and its interpretation that will need to be addressed before the paper is suitable for publication (see below).

We thank the reviewer for their comments. Following the reviewers' suggestion, we provide additional information on the bloom characteristics in the revised manuscript. While quantitative data on phytoplankton community composition is not available at this point, we have now included data on iron concentrations in our manuscript (and invited the colleagues who have conducted those measurements as co-authors). In addition to changes in the results section (P10, L26-28 & P11, L2-3), average 100 m depth-integrated total dissolved Fe concentrations have been added to Table 2 and profiles are shown in the new Figure 4. Furthermore sampling for and measurements of dissolved iron are specified in the methods section (P5, L27-33).

Other comments (some major - some minor - but in order of appearance)

Page 3 Line 34. …blooms with a putatively different iron supply.

Agreed and changed accordingly (P3, L31-34).

Page 5 Lines 15-16. What about nutrients in the upper 10 m? Why weren't they included in the deficit calculations? Since these are likely to be high in winter and lowest in summer, they could alter the nutrient deficit calculations greatly.

While we have included the upper most 10 m (0-10 m) into the deficit calculations, depths shallower than 10 m could unfortunately not be sampled by the rosette due to safety constrains (mainly because of the high swell in the area during sampling) as well as the particularly deep draft of Polarstern (about 11m). For the calculated integrals, the upper 10

m values (0-10 m) were based on data sampled at 10 m depth. To account for the reviewers comment, we have changed the sentence to "The nutrient deficit per m^3 at each station was averaged over the different depths, while the deficit per m^2 was calculated by integrating the deficits from 10-120 m data for the water column of 0-120 m." (P5, L14-16).

Line 29. What is a monkey deck?

The monkey deck is the uppermost deck of the ship, also called compass or observation deck, situated above the bridge. We have changed this to "upper-most deck" (P6, L2).

Page 7 Line 3. Are these PAR percentages relative to downwelling PAR above the ocean surface or just below the ocean surface?

These PAR percentages are relative to downwelling PAR above the ocean surface. This is now specified in the methods description (P7, L12-15).

Page 10 Top two paragraphs. Pb is not a measure of photosynthetic efficiency - it is the carbon assimilation rate or the maximum light-saturated photosynthetic rate (normalized to chl concentration). The values they report for Pb are extremely high. Most published values are below 3 (see recent compilation by Smith et al (2015)). These high values need to be explained, especially since the paper doesn't describe how these values were determined. It would be helpful to have values for the other photosynthetic parameters such as Ek and alpha (the true photosynthetic efficiency), if they are available. Also, the POC:PON ratios are quite low, well below Redfield. High detrital concentrations generally yield higher than Redfield POC:PON ratios so why are these so low? Especially since samples were collected after the peak of the bloom during its decline phase. This also needs to be addressed. It would be useful to have presented POC:Chl ratios to compare to other phytoplankton blooms. Surely, these data are available. In general, very little information about the blooms, particularly with respect to phytoplankton physiology, are presented.

The choice of abbreviation for our carbon-specific production rates, P^b, seems to have been misleading, as P^b can easily be confused with $P_m{}^b$. We are not referring to data from short-term PI curves as the referee is assuming, but to POC-normalized 24h net primary production (see methods section P7, L33 – P8, L2). Thus, there is unfortunately no data for the E_k and α available. To avoid such confusion in the future, we have changed the abbreviation used for this parameter from "P^b" to "$NPP_{Chl\ a}$" throughout the manuscript.

Data given in the publication referred to by the reviewer (1.1 ± 0.06 μg C (μg Chl)$^{-1}$ h^{-1}; Smith et al., 2015) are per hour, not per day, and they refer to maximum and not whole water column integrated values. Our data normalized per hour would be in the order of 0.4-1.3 μg C (μg Chl a)$^{-1}$ h^{-1}, which seems to be reasonable considering these are not maximal rates but water-column integrated that moreover include night-time.

We thank the reviewer for drawing our attention to the unusually low POC:PON ratios. When checking the raw data, we found an error in the calculation spread sheet. After recalculating, the POC:PON ratios are 6.3 ± 0.6 mol mol^{-1} and 5.9 ± 0.5 mol mol^{-1} for the 12°W and the 39°W bloom, respectively. The values mentioned in the results section (P10, L4-5 & L11-12) and in Table 2 were changed accordingly.

The reviewer furthermore requested POC:Chl a ratios to be added to the manuscript. In the submitted version of the manuscript, we have presented Chl a:POC ratios of both bloom areas (Table 2), i.e. the reversed ratio. Following the reviewers suggestion, we have now changed this to POC:Chl a in the revised manuscript. As these ratios do not differ between the two blooms, we think that it is sufficient to present these values in the overview Table 2.

The referee furthermore commented on the fact that very little information on phytoplankton physiology is given in the manuscript. We agree that physiological measurements would have been an interesting addition to this dataset, but unfortunately such data are not available.

Page 14. Line 3. Lower P^b doesn't indicate lower photosynthetic efficiency. It indicated lower light-saturated rates, perhaps due to nutrient limitation.

This comment seems to be linked to the confusion between $P_m{}^b$ and the P^b parameter we describe above. By changing the abbreviation to $NPP_{Chl\ a}$, we hope that this will prevent further confusion.

Lines 8-19. Si:NO3 deficits have been related to iron limitation, but no iron data were presented until line 26 of this section. It needs to be noted that differences in NO3:PO4 and Si:NO3 ratios can also be related to taxonomic differences between the blooms, especially if one has a different relative abundance of diatoms.

As mentioned above, iron data is now included in the manuscript (Figure 4, Table 2). We generally agree with the reviewer that differences in NO_3:PO_4 and Si:NO_3 deficit ratios can also be related to taxonomic differences between the blooms. As differences in NO_3:PO_4 ratios are larger than those in Si:NO_3 in the current dataset, we do not believe that the observed pattern in deficits are caused by differences in the relative abundance of diatoms. We have nonetheless added the information that taxonomic differences can affect nutrient deficit ratios to this part of the discussion (P15, L19-21).

Page 15 Line 14. Why would the bloom at 39°W be better acclimated to its environment than the bloom at 12°W?

We suggest that the 39°W bloom could be better acclimated to its environment because it putatively received a higher and steadier iron supply. This could be due to the fact that it developed within the core of a large meander (Strass et al. this issue), that recurrently forms north of South Georgia (Borrione & Schlitzer, 2013) and seems to support a shallower mixed layer, which in turn may allow for improved photoacclimation. We have now specified these aspects in the respective paragraph (P16, L24-26).

Line 27-28. Net production (if they mean net primary production) is gross production minus phytoplankton respiration. It does not depend on zooplankton grazing rates.

While we agree with the reviewer that by definition net primary production is gross production minus phytoplankton respiration, the measured values for this parameter will still depend on realistic phytoplankton biomass accumulation over the 24-hour measurement period, which will be strongly altered by loss terms such as grazing, even though respiration by grazers is not accounted for.

Page 16. Line 12. The fact that these were diatom-dominated blooms needs to be mentioned earlier. Data on relative abundances of diatoms versus other taxa should also be presented.

We agree and have now already mentioned the fact that these were diatom-dominated blooms in the general bloom description in the results section of the revised manuscript (P9, L13-14). Unfortunately, quantitative data on phytoplankton community composition is not available at this point, but we have added information of qualitative analysis to the methods section (P6, L33-34).

Line 31. How can iron availability play a pivotal role in the phytoplankton bloom if the bloom is under top-down control, as the authors argue earlier on this page?

As we argue in the manuscript we believe that "bottom-up processes might control the rate of build-up of a bloom, while top-down processes seem to be more important for determining the phytoplankton standing stock at the late bloom stage, i.e. when sampling took place" (P18, L3-5). We have specified this by changing the sentence to "iron supply seems to be the bottom-up process playing a pivotal role, particularly for determining bloom development and its potential duration, but also by modulating the light-use efficiency of phytoplankton (Smetacek et al. 2012, Behrenfeld and Milligan 2013)." (P18, L10-13).

Reviewer #2:

General comments

The sites at 39°W and 12°W differ in mixed layer depths, which are deeper at the latter. The authors do not show or discuss how the euphotic layer extends with depth at these locations (no water column PAR profile data are given; they should though). It is likely (?) that the euphotic depth (0.8% PAR) is confined within the MLD at 12°W but extends deeper than the MLD at 39°W. This is of importance and needs to be discussed, as it relates with the likely occurrence of shallow nitrification (see Smart et al. GBC, 29, 2015). In case the Zeu is < MLD any nitrification in the low PAR depth range will provide locally produced nitrate available for phytoplankton circulating within the ML. Such a condition will decrease the true NO3 deficit (<DELTA>NO3) and thus the <DELTA>Si(OH)4/<DELTA>NO3 deficit ratio (which will increase). With a shallower MLD at 39°W, nitrification at low PAR possibly occurs below the MLD, and so that nitrate would not be available for uptake by ML phytoplankton. This could partly explain the larger <DELTA>Si(OH)4/<DELTA>NO3 deficit ratio at 12°W. Apparently the nitrification effect (if indeed existing) overwhelms any inverse effect higher Si uptake under Fe limiting conditions would have on the <DELTA>Si(OH)4/<DELTA>NO3 deficit ratio. It remains of course puzzling that nitrate deficit differences between sites are not that large, despite differences in duration of the bloom at the time of sampling. High lateral inputs at 39°W might indeed be the explanation. Close inspection of profiles of nitrite and ammonium in the upper water column might provide indications of the depth region where ammonification-nitrification is ongoing at both sites. In any case authors should provide information about ammonium, nitrite concentrations and discuss this against the possible impact any shallow nitrification would have on their conclusions.

First of all, we would like to thank the reviewer for providing her/his interesting new perspective on our data. For some stations light profiles have indeed been measured (n=6+1

from 12°W+39°W bloom regions, Cheah et al. unpubl. results), the depth of 0.8% surface irradiance was estimated to range between 21 and 35m depth at all stations. These results are now reported in the manuscript (P10, L14-17). With the exception of station PS79/149, where the MLD was only 12m, all MLDs are deeper than the euphotic zone, i.e. shallow nitrification in the low PAR depth could have influenced nitrate concentrations in both areas. In the study referred to by the reviewer (Smart et al. 2015, GBC), it is explicitly stated that significant nitrification only takes place in the winter mixed layer, but not in summer. We therefore assume that this process should not have a significant effect on our deficit calculations. In agreement with this, nitrite profiles indicate maximal concentrations at the bottom of the mixed layer. Unfortunately, ammonia concentrations were not measured during the cruise, but nitrite average profiles have been added to Figure 2 to account for the reviewers comment. Furthermore, we have added a sentence to the respective paragraph stating that "while shallow nitrification has been shown to influence SO nitrate concentrations in winter, it does not seem to influence nutrient concentrations and deficits in summer (Smart et al. 2015, cf. nitrate profiles in Figure 2)" (P15, L22-24).

Specific comments

Page 4, Line 6: in case the results for the 121 stations sampled along 10°E are not discussed in this paper, why mentioning these?

We agree with the referee that this information is not necessary and have thus omitted this half-sentence (P4, L4-6).

Page 11, Lines 30-34: The productivities mentioned are similar to those measured in the same area along 6°W (same latitudes) during early season 1992. See paper by Jochem et al. (1995) in Polar Biology, 15. That paper should be mentioned.

We thank the reviewer for this suggestion and have added the information and reference to the respective part of the discussion (P12, L33 – P13, L2).

Page 15, Line 22: Dynamic currents and associated nutrients will affect similarly nutrients and DIC ..

We agree with the reviewer that dynamic currents can affect both nutrient and DIC inventories. As DIC deficits establish on shorter timescales than those of nutrient, we still believe that our statement regarding export efficiencies is valid.

Page 16, line 24 (typos) : .. processes might to control ..;

We thank the reviewer for pointing out this typo and have changed the text accordingly.

Line 27: .. we did not significant ..

Agreed and corrected.

Table 1: Add info on ZTmin and Zeu

As stated in the methods section, Z_{tmin} was 150 ±15m at all stations. We did not use this abbreviation (P5, L20-22), but have included in the results section of the revised version of the manuscript. As Z_{eu} does not provide any information on the reasons for the similarities

and differences between both bloom areas we would refrain from adding this information to Table 1(unless urgently requested by the reviewer or the editor).

As mentioned above, light profiles were unfortunately only measured at 6 stations in the 12°W bloom area (Z_{eu} (0.8%) = 29.6 ±7.6 m) and only at one station in the 39°W bloom area (Z_{eu} (0.8%) = 21.5 m). We therefore think that it is not necessary to provide this data in the table. Instead, we have added the information to the results section by stating that "Light profiles in the surface ocean were measured at 6 stations in the 12°W bloom area (with an average depth of the euphotic zone, Z_{eu} [0.8%], of 29.6 ±7.6 m) and only one station in the 39°W bloom area (Z_{eu} [0.8%] = 21.5 m), indicating similar euphotic depths in both blooms" (P10, L14-17).

Table2: add brackets to SiOH4: Si(OH)4; last line Si/NO3 deficit is indicated as 2.0 while in text it is 1.9

We thank the reviewer for pointing out these two mistakes. We have changed the table (i.e. adding brackets) and the text (i.e. correcting the deficit value to 2.0, P11, L1) accordingly.

Controls of primary production in two phytoplankton blooms in the Antarctic Circumpolar Current

Hoppe, C.J.M.[a]*, Klaas, C.[a], Ossebaar, S.[b], Soppa, M.A.[a], Cheah, W.[a,c], Rost, B.[a], Wolf-Gladrow, D.A.[a], Bracher, A.[a,d], Hoppema, M.[a], Strass, V.[a], and Trimborn, S.[a,e]

[a]Alfred Wegener Institute - Helmholtz Centre for Polar and Marine Research, Am Handelshafen 12, 27570 Bremerhaven, Germany
[b]NIOZ - Royal Netherlands Institute for Sea Research, Landsdiep 4, 1797 SZ 't Horntje (Texel), The Netherlands
[c]Research Center for Environmental Changes, Academia Sinica, 128 Academia Road, 11529 Taipei, Taiwan
[d]Institute of Environmental Physics, University Bremen, Otto Hahn Allee 1, 28359 Bremen, Germany
[e]Marine Botany, University Bremen, Leobener Straße NW2, 28359 Bremen, Germany

* Corresponding author (Clara.Hoppe@awi.de; +49 471 4831-2096)

Abstract

The Antarctic Circumpolar Current has a high potential for primary production and carbon sequestration through the biological pump. In the current study, two large-scale blooms observed in 2012 during a cruise with *RV* Polarstern were investigated with respect to phytoplankton standing stocks, primary productivity and nutrient budgets. While net primary productivity was similar in both blooms, chlorophyll *a* –specific photosynthesis was more efficient in the bloom closer to the island of South Georgia (39°W, 50°S) compared to the open ocean bloom further east (12°W, 51°S). We did not find evidence for light being the driver of bloom dynamics as chlorophyll standing stocks up to 165 mg m^{-2} developed despite mixed layers as deep as 90 m. Since the two bloom regions differ in their distance to shelf areas, potential sources of iron vary. Nutrient (nitrate, phosphate, silicate) deficits were similar in both areas despite different bloom ages, but their ratios indicated more pronounced iron limitation at 12°W compared to 39°W. The differences in iron availability as well as grazing pressure could explain observations on different temporal scales.

Keywords: biological pump; nutrient budgets; primary productivity; Southern Ocean

1. Introduction

Oceanic phytoplankton account for about half of the global primary production, thereby providing the basis of marine food webs and exerting a major control on biogeochemical cycles and global climate (Falkowski et al. 1998, Field et al. 1998). The supply of nutrients such as nitrate, phosphate and silicate to the photic zone (i.e. 'new' nutrients) constrains the biologically-mediated export of organic carbon to the deep ocean (Dugdale and Goering 1967, Eppley and Peterson 1979, Longhurst and Harrison 1989). The strength of this biological carbon pump can be estimated from the degree to which these nutrients are consumed as well as the carbon to nutrient ratios in the organic matter sinking to depth.

One area with great potential for an increase in both new and recycled production is the Antarctic Circumpolar Current (ACC). As concentrations of nitrate and phosphate are high, primary production is limited by other controlling factors (Priddle et al. 1992, Moore et al. 2000). More specifically, productivity in the ACC region is thought to be controlled by interactions between light availability (Mitchell and Holm-Hansen 1991, Nelson and Smith 1991), iron supply (Martin 1990, de Baar et al. 1995), silicate limitation (Brzezinski et al. 2003), and the effect of grazing (Dubischar and Bathmann 1997, Atkinson et al. 2001). More recent studies suggest that iron is the primary limiting factor in these open ocean areas (Smetacek et al. 2012). Phytoplankton blooms in the ACC tend to occur downstream of land masses and have been associated with fronts, islands and bathymetric features, which increase the input of iron and other trace metals into the surface waters (Moore et al. 1999, Blain et al. 2001, Borrione and Schlitzer 2013). In the Atlantic sector of the ACC, high phytoplankton standings stocks and production rates have been observed in the Antarctic Polar Frontal Zone (APFZ; Bathmann et al. 1997, Bracher et al. 1999, Moore and Abbott 2000, Tremblay et al. 2002). In this particular region, an alleviation of light limitation through upper water column stratification in spring was proposed as a trigger for the development of phytoplankton blooms. Finally, the termination of blooms is often caused by a combination of grazing pressure as well as iron and silicate limitation (Abbott et al. 2000, Tremblay et al. 2002).

Attempts to disentangle the effects of potential factors controlling bloom dynamics are complicated by the fact that these different factors tend to co-vary and also interact with each other (e.g. iron limitation decreases photoadaptive capabilities, thereby affecting light limitation; Sunda and Huntsman 1997, Petrou et al. 2014). The aim of the present study was, therefore, to understand how different environmental factors influence the biomass, primary productivity, nutrient usage and the potential for carbon sequestration in two large-scale phytoplankton blooms with putatively different iron supply.

2. Material and methods

2.1. Cruise track and sampling locations

Sampling was conducted in the framework of the 'Eddy-Pump' project during the ANT-XXVIII/3 expedition on-board the German research vessel *Polarstern* (Wolf-Gladrow 2013). Between January and March 2012, 121 stations were sampled on a transect along 10°E between 44°S and 53°S as well as in two survey areas. During the two surveys, in addition to physical properties, nutrient and chlorophyll concentrations as well as primary productivity were determined at 10 stations in a land-remote bloom at 50 - 52°S and 13.5 - 11.5°W (hereafter 12°W bloom) and at 9 stations in a bloom downstream of South Georgia at 48 - 52°S and 37 - 39°W (hereafter 39°W bloom; Figure 1). All water samples were obtained at discrete depths (10, 20, 40, 60, 80 and 100 m) from Niskin bottles attached to a Conductivity Temperature Depth (CTD) rosette. The mixed layer depth was defined as a change of density of 0.02 kg m^{-3} relative to the uppermost value of each CTD vertical profile (Cisewski et al. 2005, Strass et al. this issue). It should be noted that at station PS79/085, chlorophyll biomass was evenly distributed to a deeper pycnocline at a depth of 82 m even though the MLD determined was 30 m only.

2.2. Nutrient measurements and nutrient deficit calculations

Macronutrients were measured colorimetrically using a Technicon TRAACS 800 auto-analyzer (Seal Analytical) on board the ship. Orthophosphate (PO_4^{3-}) was measured at 880 nm after the formation of molybdophosphate-complexes (Murphy and Riley 1962). Orthosilicate ($Si(OH)_4$) was measured at 820 nm after formation of silica-molybdenum complexes with oxalic acid being added to prevent the formation of phosphate-molybdenum (Strickland and Parsons 1968). After nitrate reduction through a copperized cadmium coil, nitrate plus nitrite ($NO_3^-+NO_2^-$) was measured at 550 nm after complexation with sulphanylamide and naphtylethylenediamine (Grasshoff et al. 1983). Complex formation without the reduction step was used to determine nitrite concentrations. Nitrate is calculated by subtracting the nitrite value from the 'NO_3+NO_2' value (Grasshoff et al. 1983).

Prior to analysis, all samples and standards were brought to 22°C in about 2 h. Concentrations were recorded in mmol m^{-3} at this temperature. Calibration standards were diluted from stock solutions of the different nutrients in 0.2 µm filtered low nutrient seawater. During every run, a freshly diluted mixed nutrient standard, containing silicate, phosphate and nitrate, the so-called 'NIOZ nutrient cocktail', was measured in triplicate. Every 2 weeks, a

sterilized 'Reference Material Nutrient Sample' (JRMNS, Kanso Technos, Japan) containing known concentrations of silicate, phosphate, nitrate and nitrite in Pacific Ocean water was analysed in triplicate. The cocktail and the JRMNS were both used to monitor the performance of the analyser. Finally, the NIOZ nutrient cocktail was used to adjust all data by multiplying with the offset factor derived from the differences between assigned and measured nutrient concentrations. The average standard deviation of the NIOZ nutrient cocktail measurements were 0.02 mmol m^{-3} for phosphate, 0.59 mmol m^{-3} for silicate and 0.13 mmol m^{-3} for nitrate (n=113).

Surface nutrient concentrations were calculated as the weighted average of the measured values for sampling depths 10 - 60 m, accounting for differences in sampling frequency with increasing depth. Nutrient deficits for each station were calculated as the differences between the nutrient concentration in remnant Antarctic Winter Water (AWW) in the layer below the seasonal pycnocline and the average concentrations above that (Jennings et al. 1984, Hoppema et al. 2000). Nutrient deficit per m^3 at each station were averaged over the different depths, while deficits per m^2 were calculated by integrating the deficits for 10 - 120 m. It should be noted that nutrient deficits are suitable estimates for annual net community production only if vertical and lateral mixing in both the temperature minimum and the surface layer are small (Jennings et al. 1984, Hoppema et al. 2000, Hoppema et al. 2007). The deficits thus represent a somewhat larger area than just the station location. The AWW layer, which was characterised by a well-defined potential temperature minimum visible in CTD profiles, was situated at 150 ± 15 m water depth during this cruise. AWW nutrient concentrations were similar in both bloom areas (2.1 ± 0.1 mmol m^{-3} for phosphate, 30.1 ± 6.1 mmol m^{-3} for silicate and 30.6 ± 1.4 mmol m^{-3} for nitrate; n=113; Figure 2). Deficit ratios (i.e. $Si(OH)_4$:NO_3 and NO_3:PO_4) were calculated after averaging the nutrient deficits from the different depths at each station.

2.3. Irradiance estimates

Solar irradiance was measured continuously at one-minute intervals using a RAMSES hyperspectral radiometer (TriOS GmbH, Germany) placed on the monkey deck of the ship to avoid shading. The sensor measured downwelling incident sunlight from 350 to 950 nm with a spectral resolution of 3.3 nm. Plane photosynthetically active radiation (PAR) was calculated as the integral of irradiances from 400 to 700 nm. Daily PAR values [mol photons m^{-2} d^{-1}] were then calculated by integrating the PAR values from the start to the end of each incubation experiment (~24 h).

2.4. Chlorophyll a

Chlorophyll *a* (Chl *a*) concentrations were determined by two methods: fluorometry (Chl a_{FLUO}) and high performance liquid chromatography (HPLC; Chl a_{HPLC}). Except for stations PS79/160 and PS79/175, where Chl a_{FLUO} data were used, Chl *a* estimates are based on Chl a_{HPLC} data. The two Chl *a* datasets produced similar results, showing a significant correlation and only minimal differences ($r^2 = 0.97$, $p < 0.001$, n=104, Chl a_{FLUO} = 0.990* Chl a_{HPLC} + 0.0837).

For the Chl a_{FLUO} determination, samples were filtered onto 25 mm diameter GF/F filters (Whatman; 0.7 µm nominal pore size) at a vacuum of <100 mmHg. Filters were immediately transferred into centrifuge tubes containing 10 mL of 90% acetone and 1 cm^3 of glass beads. The tubes were sealed and stored at -20°C for at least 30 min and up to 24 h. Chl a_{FLUO} was extracted by placing the centrifuge tubes in a grinder for 3 min followed by centrifugation at 0°C. The supernatant was poured into quartz tubes and the Chl a_{FLUO} content was quantified in a 10-AU fluorometer (Turner). Calibration of the fluorometer was carried out at the beginning and at the end of the cruise, diverging by 2%. Chl a_{FLUO} content was calculated using the equation given in Knap et al. (1996) and the average parameter values from the two calibrations.

For the Chl a_{HPLC} determinations, samples were filtered onto 25 mm diameter GF/F filters (Whatman; 0.7 µm nominal pore size) at a vacuum of <100 mmHg. Filters were shock-frozen in liquid nitrogen and stored at -80°C until analysis in the home laboratory following the method described by Hoffmann et al. (2006) as detailed in Cheah et al. (this issue). For calculating Chl a_{HPLC} the sum of concentrations of monovinyl-, divinyl chlorophyll *a* and chlorophyllide *a* was taken (divinyl chlorophyll *a* was not detected in our samples).

2.5. Particulate organic carbon and nitrogen

Samples for particulate organic carbon (POC) and nitrogen (PON) were filtered onto pre-combusted (15 h, 500°C) glass fibre filters (GF/F, Whatman). Filters were stored at -20°C and processed according to Lorrain et al. (2003). Analyses were performed using a CHNS-O elemental analyser (Euro EA 3000, HEKAtech).

2.6. Primary Productivity

Net primary production rates (NPP) were determined in duplicates by the incubation of 20 mL seawater sample spiked with 20 µCi $NaH^{14}CO_3$ (53.1 mCi $mmol^{-1}$; Perkin Elmer) in a 20 mL

glass scintillation vial for 24 h in a seawater cooled on-deck incubator. Seawater samples from 6 depths (10, 20, 40, 60, 80 and 100 m) were incubated at different irradiances, which were achieved with neutral density filters decreasing incoming PAR to 25, 12.5, 6.3, 3.1, 1.6 and 0.8%.

After the addition of the $NaH^{14}CO_3$ spike, 0.1 mL aliquots were immediately removed and mixed with 10 mL of scintillation cocktail (Ultima Gold AB, PerkinElmer). After 2 h, these samples were counted with a liquid scintillation counter (Tri-Carb 2900TR, PerkinElmer) to determine the total amount of added $NaH^{14}CO_3$ (100%). For blank determination, one additional replicate per sample was immediately acidified with 0.5 ml 6N HCl (blank). After the outdoor incubation of the samples over 24 h, ^{14}C incorporation was stopped by adding 0.5 mL 6N HCl to each vial. The vials were then left to degas overnight, thereafter 15 ml of scintillation cocktail (Ultima Gold AB) were added and samples were measured after 2 h with the same liquid scintillation counter. NPP rates [mg C m^{-3} d^{-1}] at each sample depth were calculated as follows:

$$NPP\ [mg\ C\ m^{-3}\ d^{-1}] = (DIC * (DPM_{sample} - DPM_{blank}) * 1.05) / (DPM_{100\%} * t) \quad (1)$$

where DIC is the concentration of dissolved inorganic carbon [µmol kg^{-1}], t is the incubation time [h] and 1.05 is the factor describing the discrimination between incorporation of ^{14}C and ^{12}C. DPM_{blank}, DPM_{sample} and $DPM_{100\%}$ are the disintegration per minute measured by the scintillation counter for the blank, the sample and the determination of the total amount of added $NaH^{14}CO_3$, respectively. Chl *a*-specific carbon fixation (P^b [mg C [mg Chl *a*]$^{-1}$ d^{-1}]) was calculated by dividing the depth-specific NPP value by the depth-specific Chl *a* concentrations. Column-integrated primary productivity (NPP [mg C m^{-2} d^{-1}]) and Chl *a*-specific carbon fixation (P^b [mg C (mg Chl *a*)$^{-1}$ d^{-1}]) were derived by integrating values for 100 m depth.

2.7. Satellite Chl a maps

Weekly satellite maps of Chl *a* were used to study the development of the blooms. The comparison of satellite derived Chl *a* concentrations with the in-situ values measured at the two bloom locations was based on daily maps. The Chl *a* maps were derived using the POLYMER level-3 product of the Medium Resolution Imaging Spectrometer (MERIS) at a 0.02° spatial resolution (Steinmetz et al. 2011). POLYMER is an improved atmospheric correction algorithm for pixels contaminated by sun glint, thin clouds or heavy aerosol

1 plumes. MERIS Polymer products improve the spatial coverage by almost a factor of two and
2 have been proven successful for retrieving MERIS Ocean Colour products (Müller et al.
3 2015). The Chl *a* concentrations are retrieved using the standard OC4Me algorithm (Morel et
4 al. 2007).

1 3. Results
2
3 *3.1. Temporal and spatial development of the blooms*
4 During late austral summer (January - March) 2012, two large-scale phytoplankton blooms
5 were observed in the APFZ (Figure 1A). A comparison of all surface Chl *a* concentrations
6 (<10 m) derived by HPLC measurements with daily MERIS Polymer Chl *a* within the
7 respective satellite pixel (Figure 1B, C) revealed a reasonable correlation coefficient (r^2 =
8 0.67), low bias (0.17 mg m^{-3}) and low percentage error (33%) between the two approaches.
9 Estimates of Chl *a* standing stocks from in-situ measurements and satellite-based products are
10 thus in good agreement, showing a nearly perfect match for the bloom situated at 12°W
11 (Figure 1C). A reasonable agreement was observed for the 39°W bloom north of South
12 Georgia, where satellite data tended to underestimate Chl *a* concentrations, particularly in the
13 higher range of the measured values (Figure 1B).
14 In the 12°W bloom area (Figure 1A, C), satellite Chl *a* maps indicated that a bloom
15 developed from mid December 2011 onwards and peaked in the first two weeks of January
16 2012 with Chl *a* concentrations of around 3 mg m^{-3}. Our in-situ sampling took place between
17 January 26th and February 15th, i.e. in the declining phase of the bloom. Within these three
18 weeks, a central station (at 12°6'W, 51°2'S) was re-visited six times to investigate the
19 temporal development of the bloom. The satellite data indicated that Chl *a* concentrations in
20 the area quickly decreased within 5 days after the last sampling date to values lower than 1
21 mg m^{-3}.
22 The phytoplankton bloom at 39°W (Figure 1 A, B) was located in the Georgia Basin,
23 north of the island of South Georgia. Satellite Chl *a* maps indicated that the 39°W bloom had
24 already developed during mid October and peaked in mid-December with surface Chl *a*
25 concentrations reaching values higher than 3 mg m^{-3}. In-situ sampling took place between
26 February 16th and March 3rd, in the declining phase of the bloom. Satellite data indicated that
27 Chl *a* concentrations above 0.5 mg m^{-3} persisted at least until mid March.
28
29 *3.2. Phytoplankton standing stocks and primary productivity*
30 In the 12°W area, average MLD was 71 ± 14 m. The depth-integrated Chl *a* concentrations in
31 the bloom ranged from 50 to 180 mg Chl *a* m^{-2} (Table 1) and were on average 120 ±41 mg
32 Chl *a* m^{-2}. Values were as low as 9 mg m^{-2} outside the bloom area (Table 2). NPP ranged from
33 800 to 2820 mg C m^{-2} d^{-1} (Table 1) and was on average 1750 ± 750 mg C m^{-2} d^{-1} (Table 2) in
34 the bloom, and thus significantly higher than values outside the bloom area (160 mg C m^{-2} d^{-}

^{1}). Chl *a*-specific carbon fixation P^b, a measure of photosynthetic efficiency, varied between 10.1 and 17.3 mg C [mg Chl *a*]$^{-1}$ d^{-1} (on average 14.4 ± 2.6 mg C [mg Chl *a*]$^{-1}$ d^{-1}) in the 12°W bloom (Table 1 and 2). The average depth-integrated POC:PON ratios in this area were 4.6 ± 0.4 mol mol^{-1} (Table 2). Average daily PAR during primary production measurements in the 12°W bloom was 12.3 ± 5.1 mol photons m^{-2} d^{-1} (Table 2).

In the 39°W bloom north of South Georgia, average MLD was 35 ± 13 m. In-situ Chl *a* standing stocks ranged from 25 to 130 mg Chl *a* m^{-2} (Table 1), with an average of 60 ± 30 mg Chl *a* m^{-2} (Table 2). NPP (Table 1) in this region varied between 570 and 3020 mg C m^{-2} d^{-1} (on average 1370 ± 830 mg C m^{-2} d^{-1}). P^b varied between 14.4 and 30.3 mg C [mg Chl *a*] $^{-1}$ d^{-1} (average of 19.4 ± 5.5 mg C [mg Chl *a*] $^{-1}$ d^{-1}). In the 39°W bloom, depth-integrated average POC:PON ratios (Table 2) was 4.3 ± 0.3 mol mol^{-1}. Average daily PAR during primary production measurements in this bloom was 15.7 ± 6.1 mol photons m^{-2} d^{-1} (Table 2).

3.3. Nutrient concentrations and deficits

In the area of the 12°W bloom, average surface nutrient concentrations (10 m depth) were 19.7 ± 0.3 mmol NO_3 m^{-3}, 1.3 ± 0.1 mmol PO_4 m^{-3}, and 4.1 ± 3.1 mmol $Si(OH)_4$ m^{-3} (Figure 2). The average nutrient concentrations in the euphotic zone (10 - 60 m) were 20.6 ±0.5 mmol NO_3 m^{-3}, 1.4 ±0.1 mmol PO_4 m^{-3}, and 6.6 ±2.7 mmol $Si(OH)_4$ m^{-3} (Table 2). Average integrated nutrient deficits in this area were 1090 ± 110 mmol NO_3 m^{-2}, 75 ± 7 mmol PO_4 m^{-2}, and 2710 ± 300 mmol $Si(OH)_4$ m^{-2} (Table 2) with a $Si(OH)_4$:NO_3 deficit ratio of 2.5 ± 0.3 mol mol^{-1} and a NO_3:PO_4 deficit ratio of 14 ± 1 mol mol^{-1} (Table 2, Figure 3).

In the 39°W bloom area, average surface nutrient concentrations (10 m depth) were 14.9 ± 1.8 mmol NO_3 m^{-3}, 1.0 ± 0.1 mmol PO_4 m^{-3}, and 0.6 ± 0.5 mmol $Si(OH)_4$ m^{-3} (Figure 2). Average nutrient concentrations of the euphotic zone (10 - 60 m) were 16.3 ± 1.8 mmol NO_3 m^{-3}, 1.2 ± 0.1 mmol PO_4 m^{-3} and 2.2 ± 1.3 mmol $Si(OH)_4$ m^{-3} (Table 2). Resulting average integrated surface nutrient deficits in the 39°W bloom area were 1220 ± 310 mmol NO_3 m^{-2}, 68 ± 18 mmol PO_4 m^{-2} and 2360 ± 630 mmol $Si(OH)_4$ m^{-2} (Table 2), resulting in $Si(OH)_4$:NO_3 deficit ratios of 1.9 ± 0.4 mmol mmol^{-1} and NO_3:PO_4 deficit ratios of 17 ± 1 mmol mmol^{-1} in this region (Table 2, Figure 3).

Due to the high variability within each bloom, no significant differences in nutrient concentrations or deficits were detectable between the two study areas (Table 2). The ratios of $Si(OH)_4$:NO_3 deficits, however, were significantly lower in the 39°W area compared to the 12°W bloom (t-test, t = 6.6, p <0.001, n = 35 + 26; Table 2, Figure 3), while the ratios of NO_3:PO_4 deficits were significantly higher at 39°W (t-test, t =15.4, p <0.001, n = 35 + 26).

4. Discussion

4.1. High variability of primary productivity in the APFZ

During the present cruise, two large-scale phytoplankton blooms in the Atlantic sector of the ACC were observed (Figure 1). Both blooms were located between 50°S and 52°S in the APFZ. Phytoplankton blooms are regularly observed in this region during spring and summer (e.g. Laubscher et al. 1993, Bathmann et al. 1997, Bracher et al. 1999, Tremblay et al. 2002). The occurrence of blooms in SO frontal zones has been associated with their oceanographic features such as jet streams, meanders and mesoscale eddies, which can lead to increased iron and silicate supply by mesoscale upwelling but also enhanced stratification due to cross-frontal overlayering (de Jong et al. 1998, Bracher et al. 1999, Strass et al. 2002a, Tremblay et al. 2002), thereby alleviating nutrient and light limitation for phytoplankton growth. In the Georgia Basin, bloom initialization is thought to be mainly driven by iron input from South Georgia, while further east more complex modes of iron supply generate a larger degree of spatial and temporal variability in productivity (Venables and Meredith 2009).

Being a relatively productive area within the otherwise HNLC (high-nutrient low-chlorophyll) region, the APFZ has been the destination of several research cruises (e.g. Bracher et al. 1999, Strass et al. 2002c, Tremblay et al. 2002, Korb and Whitehouse 2004). Estimates of primary productivity in the APFZ vary between 100 and 6000 mg C m^{-2} d^{-1} (Mitchell and Holm-Hansen 1991, Bracher et al. 1999, Moore and Abbott 2000, Strass et al. 2002b, Tremblay et al. 2002, Hiscock et al. 2003, Vaillancourt et al. 2003, Korb and Whitehouse 2004, Park et al. 2010), with the highest values being observed in the vicinity of land masses. The values observed in the present study are highly variable (about 160 - 3020 mg C m^{-2} d^{-1}; Table 1), but fall within the previously reported range. Antarctic phytoplankton productivity in this region has been reported to exhibit strong spatial (Veth et al. 1992, Arrigo et al. 1998), seasonal (Smith et al. 2000, Hiscock et al. 2003) and inter-annual variations (Clarke and Leakey 1996, Park et al. 2010). Sporadic and patchy sampling during research cruises makes it therefore difficult to estimate the specific productivity in this region. These sampling opportunities are nonetheless useful to investigate the variability of productivity.

During sampling in the 12°W bloom, one station in the initial centre of the bloom was investigated over a 2 week period (Figure 1, Table 1). Primary productivity estimates at this central sampling station varied between 1050 and 2820 mg C m^{-2} d^{-1} (Table 1). These values are considerably higher than previous estimates for this region (Bracher at al. 1999, Strass et al. 2002b, Tremblay et al. 2002, Korb and Whitehouse 2004). The observed temporal

variability, which was somewhat lower than the spatial variability in the 12°W region (800 – 2820 mg C m^{-2} d^{-1}, Table 1), probably reflects a combination of the changes in light availability due to cloud cover (between 5 and 20 mol photons m^{-2} d^{-1}; Table 1) as well as the movement of water masses (Strass et al. this issue). The developmental phase of the phytoplankton bloom was also an important factor as primary production decreased over time (Table 1). During the investigation of the 39°W bloom, emphasis was put on the spatial variability in productivity (Figure 1, Table 1). In this bloom, primary productivity varied slightly more compared to the first area (570 - 3020 mg C m^{-2} d^{-1}; Table 1). This may be due to the higher spatial coverage, but also temporal aspects and the more dynamic currents play a role in this area (Strass et al. this issue). Nonetheless, even at three consecutive stations sampled on the same day (PS79/168-70) and within half a degree distance to each other, primary productivity varied between 790 and 2220 mg C m^{-2} d^{-1} (Table 1), demonstrating significant small-scale variability in the 39°W bloom area (Leach et al. this issue).

The high spatial and temporal variability emphasises once more the difficulties in estimating the productivity in this highly dynamic region (Abbott et al. 2000). Even though satellite Chl *a* estimates have drawbacks compared to in-situ measurements (Schlitzer 2002, Korb and Whitehouse 2004, Whitehouse et al. 2008), they provide higher spatial and temporal coverage of phytoplankton biomass at mesoscale resolution. The satellite Chl *a* from the MERIS Polymer-Chl-product used in this study has been validated globally and regionally within the current *ESA Climate Change Initiative for Ocean colour* and was chosen as the best algorithm for MERIS data processing (Müller et al. 2015). Also in the current study, the quality of the satellite Chl *a* data (r^2 = 0.67, bias = 0.17 mg m^{-3} compared to in-situ measurements) is sufficient to analyse the development of the two phytoplankton blooms at the surface. As satellite Chl *a* data only cover the ocean's first optical depth, estimates on primary productivity can only be derived using a model that incorporates satellite-based estimates of Chl *a*, sea surface temperature and PAR to reconstruct productivity over the entire mixed layer (e.g. Antoine and Morel 1996). Shipboard Chl *a* and primary productivity data are therefore necessary in order to confirm satellite-derived products and to give information on the layers below the first optical depth. ^{14}C-based estimates tend to overestimate primary productivity due to the exclusion of loss terms such as sinking or grazing as well as biases in applied irradiances (e.g. Gall et al. 2001). Nonetheless, this method can be used to investigate the underlying mechanisms for the patterns observed in satellite-derived maps.

4.2. Patterns in primary productivity do not correlate with MLDs

In the following, the two blooms are compared based on their general characteristics rather than investigating differences between single stations because relationships with the environmental conditions have to be considered on a wider scale, especially in such a highly dynamic region as the ACC.

In terms of depth-integrated primary productivity, no significant differences between the two blooms were observed during our visit (1750 ± 750 versus 1370 ± 830 mg C m^{-2} d^{-1}, t-test: t = 1.0, p = 0.315; Tables 1 and 2). Similar rates of primary productivity were achieved even though MLDs were significantly deeper in the 12°W compared to the 39°W bloom (71 ± 14 versus 35 ± 13 m, t-test: t = 6.0, p <0.001; Table 2). Hence, despite spending different proportions of the day in the deep low-light environment, phytoplankton communities of both blooms established similar primary productivity (Figure 4A; linear regression: $r^2 = 0.208$, p = 0.05). This finding is somewhat surprising, as earlier studies suggested that the alleviation from light limitation through shoaling MLDs is a key determinant of bloom development and productivity in the open SO (Sambrotto and Mace 2000, van Oijen et al. 2004, de Baar et al. 2005). In the current study, depth-integrated Chl *a* concentrations were positively correlated with MLD over the entire study area (Figure 4B). As Chl *a*:POC ratios were similar in both blooms (Table 2), this indicated that Chl *a* as well as biomass build-up was not light limited in MLDs up to 90 m (Figure 4A; linear regression: r^2 0.568, p = 0.0002). In fact, depth-integrated primary productivity was best correlated with depth-integrated Chl *a* concentrations (Figure 4C; linear regression: $r^2 = 0.718$, p < 0.0001). Indicating that overall, phytoplankton cells were able to acclimate to different light regimes and thus sustained similar depth-integrated primary productivity at different MLDs.

It should be kept in mind, however, that the controlling role of light may be particularly important early in the growing season when deep surface mixing occurs, light availability is limited, and phytoplankton biomass is low (Bracher et al. 1999, Franck et al. 2000, Smith et al. 2000, Landry et al. 2002, Llort et al. 2015). The effects of light might explain the earlier onset of the 39°W bloom (e.g. by stratification of the upper mixed layer), while the constant iron supply from South Georgia could have caused its longer duration. The light regime at the beginning of the growing season therefore may play an important role in modulating bloom dynamics by changing the rate and duration of biomass accumulation during the build-up phase of the bloom. Even though primary productivity did not differ between blooms, the depth-integrated photosynthetic efficiencies derived from Chl *a*-specific

carbon fixation (P^b) were higher in the 39°W bloom compared to the 12°W bloom area (t-test, $t = 2.5$, $p = 0.027$). In the more deeply mixed 12°W bloom stations, lower P^b-values indicate that phytoplankton photosynthesis was less efficient (Behrenfeld et al. 2008), possibly due to a combination of lower iron availability and deeper mixing regimes. Integrated over the water column, however, this did not lead to lower productivity than in the 39°W bloom.

4.3. Nutrient deficits indicate differences in iron availability over the growing season

During the growing season, phytoplankton take up and export nutrients to a certain degree as part of particulate organic matter, which can be expressed as nutrient deficits or depletions (Le Corre and Minas 1983, Jennings et al. 1984; Table 2). These proxies for net community production as well as their ratios differed between the two bloom areas (Figure 3). While the ratios of $Si(OH)_4$:NO_3 deficits were significantly higher in the 12°W compared to the 39°W bloom area (t-test, $t = 6.6$, $p < 0.001$), the opposite trend was observed with respect to the NO_3:PO_4 deficit ratios (t-test: $t = 15.4$, $p < 0.001$). As phytoplankton need iron for the assimilation of nitrate, and to a lesser degree of phosphate, its absence leads to lowered uptake capacities (de Baar et al. 1997, Hutchins and Bruland 1998). Our results therefore indicate differences in the nutrient assimilation histories of the two phytoplankton assemblages, which might be explained by differences in magnitude and dynamics of iron supply in the two regions.

Drifter buoy trajectories indicate that water masses in the 39°W sampling region originate from the South Georgia shelf (Meredith et al. 2003), which most likely receives a higher and steadier supply of iron and other trace metals (Korb and Whitehouse 2004, Nielsdóttir et al. 2012, Borrione and Schlitzer 2013). In the area around 12°W, however, trace metal supply is thought to be restricted to deep-mixing during winter (Venables and Meredith, 2009). During the time of sampling, iron measurements in the upper 100 m of the water column yielded similarly low dissolved (0.1-0.2 µmol m^{-3}) and leachable particulate iron concentrations (0.2-0.8 µmol m^{-3}) in both areas (Laglera et al. 2013, L. Laglera, unpubl. results), indicating iron depletion in both blooms. Given the development and intensity of the blooms as inferred from satellite data, iron concentrations must have been much higher at the onset of the blooms, yet they were already depleted by phytoplankton activity and particle scavenging at the time of sampling. Despite potentially large differences in iron availability and supply, surface silicate concentrations were similarly low in both areas and could potentially limit diatom growth (Figure 2; Nelson et al. 2001). Furthermore, nutrient deficits were also similar even though phytoplankton accumulation started earlier in the 39°W area (this study, Borrione and

Schlitzer 2013). These similarities of the two blooms can partly be explained by the lower $Si(OH)_4$:NO_3 assimilation ratios at 39°W (Table 2), but may also suggest differences in the intensity of nutrient cycling, export and grazing pressure between the two systems.

4.4. From bottom-up towards top-down controls

Nutrient deficits can be used to estimate season-integrated net community production and are thus a proxy for new production on an annual basis (Jennings et al. 1984, Strass and Woods 1991, Hoppema et al. 2000, Whitehouse et al. 2012). Production rates calculated from nutrient deficits, however, can potentially be biased by altered nutrient concentrations due to vertical or lateral mixing and advection, alternative nutrient sources (e.g. ammonium), as well as changes in stoichiometry of organic matter (Jennings et al. 1984, Hoppema et al. 2007, Whitehouse et al. 2012). In agreement with Laubscher et al. (1993), slightly stronger nutrient depletion in the 39°W region co-occurred with higher photosynthetic efficiencies compared to 12°W (Table 2), indicating a better acclimation to their environment in the former bloom. The estimates of primary productivity and POC:PON as well as Chl *a*:POC ratios (Table 1 and 2), however, were in a similar range for both blooms. Furthermore, nutrient deficits, though somewhat lower in the 12°W bloom region, were not remarkably different between regions (Figure 3, Table 2). This is surprising, in particular in view of the almost two months earlier onset of the bloom in the Georgia Basin.

This apparent contradiction could have been caused by lower export efficiencies in the 39°W bloom. Shipboard carbonate chemistry measurements, however, revealed higher deficits in dissolved inorganic carbon (DIC) and a stronger CO_2 uptake from the atmosphere in the 39°W compared to the 12°W bloom area (Jones et al. this issue). Therefore, the mismatch between nutrient deficits and bloom dynamics (as observed via satellites) was more likely caused by the highly dynamic currents in the 39°W area (Strass et al. this issue), which may have led to an underestimation of seasonal nutrient deficits due to higher lateral nutrient input (Oschlies 2002). Furthermore, net productivity may have been overestimated to different degrees in both blooms because loss terms such as grazing tend to be underestimated in ^{14}C-based measurements (e.g. Gall et al. 2001).

Recent field-, satellite- and model-based studies have highlighted the thus-far underestimated importance of top-down control mechanisms for phytoplankton bloom dynamics (e.g. Behrenfeld and Boss 2014, Llort et al. 2015). As the average zooplankton biomass in the South Georgia area is larger than anywhere else in the Southern Ocean (Atkinson et al. 2001), we speculate that during the time of sampling, top-down control was

more strongly developed in the 39°W compared to the 12°W bloom area. Zooplankton sampling during our cruise showed that, despite high spatial variability, the zooplankton community around 39°W was in a more progressed state of development compared to the 12°W bloom area. In the latter, the proportion of small organisms and early developmental stages was higher (E. Pakomov and B. Hunt, unpubl. data). A potentially lower grazing pressure in the 12°W bloom could also be explained by a lower probability for predator-prey encounters in deeper MLDs (Behrenfeld 2010). In fact, this dilution effect on grazing rates might have contributed to the positive correlation between biomass and MLD found throughout our study (Figure 4B).

As the control of phytoplankton bloom dynamics in the ACC can shift from bottom-up to mainly top-down within a few weeks (Abbott et al. 2000, Llort et al. 2015), also a slightly earlier bloom development at 39°W could have led to our observations. Diatom-dominated blooms, as observed in this study (C. Klaas, unpubl. results; also indicated by silicate depletion in the surface waters, Figure 2), are mainly grazed by larger zooplankton. One can therefore assume that the usual time lag between bloom and grazer development (Smetacek et al. 2004) was still allowing phytoplankton biomass build-up in the 12°W area, while grazers already imposed a strong control on the 39°W bloom during the time of sampling. Satellite Chl *a* maps of the two bloom areas indeed show that the 39°W bloom developed around 8 weeks earlier than the 12°W bloom. We thus conclude that, despite both being in the apex phase, we visited the two areas at different stages of the bloom development.

5. Conclusions and biogeochemical implications

The results of this study suggest that a combination of different drivers strongly affect primary productivity in the SO. Bottom-up processes might to control the rate of build-up of a bloom, while top-down processes seem to be more important for determining the phytoplankton standing stock at the late bloom stage, i.e. when sampling took place (Figure 5). In contrast to earlier suggestions (van Oijen et al. 2004, de Baar et al. 2005) we did not significant light limitation of phytoplankton communities in two highly productive open-ocean areas of the Atlantic sector of the SO. Indeed, our results indicate that light limitation caused by MLDs as deep as at least 90 m does not necessarily prevent the development of phytoplankton blooms in the APFZ. Instead, iron availability seems to play a pivotal role (particularly for determining bloom duration), also by modulating the light-use efficiency of phytoplankton (Smetacek et al. 2012, Behrenfeld and Milligan 2013). Considering the time

1 scales of the individual measurements we were able to explain the observed patterns by
2 differences in iron availability and grazing pressure.

Acknowledgements

We would like to thank all scientists as well as the captain, officers and crew of RV *Polarstern* for their work and support during the ANT-XXVIII/3 cruise. Especially, we would like to thank L. Laglera, E. Jones and M. Iversen for helpful discussions on the present dataset. We thank S. Wiegmann for help with the HPLC analysis, F. Steinmetz (HYGEOS) for supplying Polymer-MERIS CHL data and ESA for MERIS level-1 satellite data. We also thank E. Jones for providing DIC measurements. Furthermore, we would like to thank F. Altvater, D. Kottmeier, R. Kottmeier, T. Rueger, V. Schourup-Kristensen for their help during the cruise as well as A. Terbrüggen, K.-U. Richter and U. Richter for help with the cruise preparations. C.J.M.H. and B.R. were funded by the European Research Council (ERC) under the European Community's Seventh Framework Programme (FP7 / 2007-2013), ERC grant agreement no. 205150. S.T. was funded by the German Science Foundation (DFG), project TR 899/2 and the Helmholtz Impulse Fond (HGF Young Investigator Group EcoTrace). Funding to M.S. was supplied by CAPES, Brazil, and to A.B. by the Helmholtz Innovation Fund Phytooptics. M.H. was supported through EU FP7 project CARBOCHANGE, which received funding from the European Community's Seventh Framework Programme under grant agreement no. 264879. This work was furthermore supported by the DFG in the framework of the priority programme "Antarctic Research with comparative investigations in Arctic ice areas" by a grant HO 4680/1.

References

Abbott MR, Richman JG, Letelier RM, Bartlett JS (2000) The spring bloom in the Antarctic polar frontal zone as observed from a mesoscale array of bio-optical sensors. Deep-Sea Research Part II: Topical Studies in Oceanography 47:3285-3314

Antoine D, Morel A (1996). Oceanic primary production: I. Adaptation of a spectral light-photosynthesis model in view of application to satellite chlorophyll observations, Global Biogeochemical Cycles 10:43-55

Arrigo KR, Worthen D, Schnell A, Lizotte MP (1998) Primary production in Southern Ocean waters. Journal of Geophysical Research: Oceans 103:15587-15600

Atkinson A, Whitehouse MJ, Priddle J, Cripps GC, Ward P, Brandon MA (2001) South Georgia, Antarctica: A productive, cold water, pelagic ecosystem. Marine Ecology Progress Series 216:279-308

Bathmann UV, Scharek R, Klaas C, Dubischar CD, Smetacek V (1997) Spring development of phytoplankton biomass and composition in major water masses of the Atlantic sector of the Southern Ocean. Deep-Sea Research Part II: Topical Studies in Oceanography 44:51-67

Behrenfeld MJ (2010) Abandoning Sverdrup's Critical Depth Hypothesis on phytoplankton blooms. Ecology 91: 977-989

Behrenfeld MJ, Halsey KH, Milligan AJ (2008) Evolved physiological responses of phytoplankton to their integrated growth environment. Philosophical Transactions of the Royal Society B: Biological Sciences 363:2687-2703

Behrenfeld MJ, Milligan AJ (2013) Photophysiological Expressions of Iron Stress in Phytoplankton. Annual Review of Marine Science 5: 217-246

Behrenfeld MJ, Boss ES (2014) Resurrecting the ecological underpinnings of ocean plankton blooms. Annual Review of Marine Science 6: 167-194

Blain S, Tréguer P, Belviso S, Bucciarelli E et al. (2001) A biogeochemical study of the island mass effect in the context of the iron hypothesis: Kerguelen islands, Southern Ocean. Deep-Sea Research Part I: Oceanographic Research Papers 48:163-187

Borrione, I, Schlitzer R (2013) Distribution and recurrence of phytoplankton blooms around South Georgia, Southern Ocean. Biogeosciences 10:217-231

Boyd PW (2002) Environmental factors controlling phytoplankton processes in the Southern Ocean. Journal of Phycology 38:844-861

Boyd PW, Ellwood MJ (2010) The biogeochemical cycle of iron in the ocean. Nature Geoscience 3:675-682

Bracher AU, Kroon BMA, Lucas MI (1999) Primary production, physiological state and composition of phytoplankton in the Atlantic sector of the Southern Ocean. Marine Ecology Progress Series 190: 1-16

Brzezinski MA, Dickson M-L, Nelson DM, Sambrotto R (2003) Ratios of Si, C and C uptake by microplankton in the Southern Ocean. Deep-Sea Research Part II: Topical Studies in Oceanography 50:619-633

Buesseler KO, Boyd PW (2009) Shedding light on processes that control particle export and flux attenuation in the twilight zone of the open ocean. Limnology and Oceanography 54: 1210-1232

Cheah W, et al. (submitted) Structure and physiological state of phytoplankton community in the Southern Ocean along a transect at 10° E, this issue.

Cisewski B, Strass VH, Prandke H (2005) Upper-ocean vertical mixing in the Antarctic Polar Front Zone. Deep Sea Research Part II: Topical Studies in Oceanography 52:1087-1108

Clarke A, Leakey RJ (1996) The seasonal cycle of phytoplankton, macronutrients, and the microbial community in a nearshore antarctic marine ecosystem. Limnology and Oceanography 41:1281-1294

Coale, KH, et al. (2004) Southern Ocean Iron Enrichment Experiment: Carbon cycling in high- and low-Si waters. Science 304:408-414

de Baar H, Boyd P, Coale K, Landry M, Tsuda A et al. (2005) Synthesis of iron fertilization experiments: From the iron age in the age of enlightenment. J Geophys Res Oceans 110: C09S16

de Baar HJW, de Jong JTM, Bakker DCE, Loscher BM, Veth C, Bathmann U, V. Smetacek V (1995) Importance of iron for plankton blooms and carbon dioxide drawdown in the Southern Ocean. Nature 373:412-415

de Baar HJW, Van Leeuwe MA, Scharek R, Goeyens L, Bakker KMJ, Fritsche P(1997) Nutrient anomalies in *Fragilariopsis kerguelensis* blooms, iron deficiency and the nitrate/phosphate ratio (A. C. Redfield) of the Antarctic Ocean. Deep-Sea Research Part II: Topical Studies in Oceanography 44:229-260

de Jong JTM, den Das J, Bathmann U, Stoll MHC, Kattner G, Nolting RF, de Baar HJW (1998) Dissolved iron at subnanomolar levels in the Southern Ocean as determined by ship-board analysis. Analytica Chimica Acta 377:113-124

Dubischar CD, Bathmann UV (1997) Grazing impact of copepods and salps on phytoplankton in the Atlantic sector of the Southern Ocean. Deep-Sea Research Part II: Topical Studies in Oceanography 44:415-433

Dugdale RC, Goering JJ (1967) Uptake of new and regenerated forms of nitrogen in primary productivity. Limnology and Oceanography 12:196–206

Eppley RW, Peterson BJ (1979) Particulate organic matter flux and planktonic new production in the deep ocean. Nature 282: 677-680

Falkowski PG, Barber RT, Smetacek V (1998) Biogeochemical controls and feedbacks on ocean primary production. Science 281:200-206

Field CB, Behrenfeld MJ, Randerson JT, Falkowski P (1998) Primary production of the biosphere: Integrating terrestrial and oceanic components. Science 281:237-240

Gall MP, Strzepek R, Maldonado M, Boyd PW (2001) Phytoplankton processes. Part 2: Rates of primary production and factors controlling algal growth during the Southern Ocean iron release experiment (soiree). Deep-Sea Research Part II: Topical Studies in Oceanography

48:2571-2590

Grasshoff K, Kremling K, Ehrhardt M (1999) Methods of Seawater Analysis, Weinheim, Wiley-VCH

Hiscock MR, Marra J, Smith WO, Goericke R et al. (2003) Primary productivity and its regulation in the pacific sector of the Southern Ocean. Deep-Sea Research II 50:533-558

Hoffmann LJ, Peeken I, Lochte K, Assmy P, Veldhuis M (2006) Different reactions of Southern Ocean phytoplankton size classes to iron fertilization, Limnology andOceanography 51: 1217-1229

Hoppema M, Goeyens L, Fahrbach E (2000) Intense nutrient removal in the remote area off Larsen Ice Shelf (Weddell Sea). Polar Biology 23:85-94

Hoppema M, Middag R, de Baar HJW, Fahrbach E, van Weerlee EM, Thomas H (2007) Whole season net community production in the Weddell Sea. Polar Biology 31:101-111

Hutchins D, Bruland K (1998) Iron-limited diatom growth and Si:N uptake ratios in a coastal upwelling regime. Nature 393:561

Jennings JC, Gordon LI, Nelson DM (1984) Nutrient depletion indicates high primary productivity in the Weddell Sea. Nature 309:51-54

Jones EM, Hoppema M, Strass V, Hauck J, Salt L, Klaas C, van Heuven SMAC, Wolf-Gladrow D, de Baar HJW (submitted): Mesoscale features create hotspots of carbon uptake in the Antarctic Circumpolar Current. This issue

Knap A, Michaels A, Close HD, Dickson A (1996) Protocols for the joint global ocean flux study (JGOFS) core measurements. UNESCO

Korb RE, Whitehouse M (2004) Contrasting primary production regimes around South Georgia, Southern Ocean: Large blooms versus high nutrient, low chlorophyll waters. Deep-Sea Research Part I: Oceanographic Research Papers 51:721-738

Laglera LM, Santos-Echeandía J, Caprara S, Monticelli D (2013) Quantification of Iron in Seawater at the Low Picomolar Range Based on Optimization of Bromate/Ammonia/ Dihydroxynaphtalene System by Catalytic Adsorptive Cathodic Stripping Voltammetry. Analytical Chemistry 85:2486-2492

Landry MR, Selph KE, Brown SL, Abbott MR et al. (2002) Seasonal dynamics of phytoplankton in the Antarctic polar front region at 170 °W. Deep-Sea Research Part II: Topical Studies in Oceanography 49:1843-1865

Leach, H, Strass, V, Prandke, H (submitted) Mixing and Finescale Structures in two Mesoscale Features of the Antarctic Circumpolar Current. This issue

Laubscher RK, Perissinotto R, McQuaid CD (1993) Phytoplankton production and biomass at frontal zones in the Atlantic sector of the Southern Ocean. Polar Biology 13:471-481

Le Corre P, Minas HJ (1983) Distributions et évolution des éléments nutritifs dans le secteur indien de l'Océan Antarctique en fin de période estivale. Oceanologica Acta 6:365-381

Llort J, Lévy M, Sallée J-B, Tagliabue A (2015) Onset, intensification, and decline of phytoplankton blooms in the Southern Ocean. ICES Journal of Marine Science: Journal du

Conseil (in press)

Longhurst AR, Glen Harrison W (1989) The biological pump: Profiles of plankton production and consumption in the upper ocean. Progress in Oceanography 22:47-123

Lorrain A, Savoye N, Chauvaud L, Paulet Y-M, Naulet N (2003) Decarbonation and preservation method for the analysis of organic C and N contents and stable isotope ratios of low-carbonated suspended particulate material. Analytica Chimica Acta 491:125-133

Martin JH (1990) Glacial-interglacial CO_2 change: The iron hypothesis. Paleoceanography 5:1-13

Meredith MP, Watkins JL, Murphy EJ, Cunningham NJ et al. (2003) An anticyclonic circulation above the northwest Georgia Rise, Southern Ocean. Geophysical Research Letters 30:GL018039

Mitchell BG, Holm-Hansen O (1991) Observations and modeling of the Antarctic phytoplankton crop in relation to mixing depth. Deep-Sea Research 38:981-1007

Moore JK, Abbott MR (2000) Phytoplankton chlorophyll distributions and primary production in the southern ocean. Journal of Geophysical Research: Oceans 105:28709-28722

Moore JK, Abbott MR, Richman JG, Nelson DM (2000) The Southern Ocean at the last glacial maximum: A strong sink for atmospheric carbon dioxide. Global Biogeochem Cycles 14:455-475

Moore JK, Abbott MR, Richman JG, Smith WO et al. (1999) SeaWiFs satellite ocean color data from the Southern Ocean. Geophysical Research Letters 26:1465-1468

Morel A, Huot Y, Gentili B, Werdell PJ, Hooker SB, Franz BA (2007) Examining the consistency of products derived from various ocean color sensors in open ocean (Case 1) waters in the perspective of a multi-sensor approach. Remote Sensing of Environment 111: 69-88

Müller D, Krasemann H, Brewin RJW, Brockmann C, Deschams P-Y, et al. (2015) The Ocean Colour Climate Change Initiative: II. Spatial and temporal homogeneity of satellite data retrieval due to systematic effects in atmospheric correction processors. Remote Sensing of Environment (in press)

Murphy J, Riley JP (1962) A modified single solution method for the determination of phosphate in natural waters. Analytica Chimica Acta 27:31-36

Nelson DM, Brzezinski MA, Sigmon DE, Franck VM (2001) A seasonal progression of Si limitation in the pacific sector of the Southern Ocean. Deep-Sea Research Part II: Topical Studies in Oceanography 48:3973-3995

Nelson DM, Smith WOJ (1991) Sverdrup revisited: Critical depths, maximum chlorophyll levels, and the control of Southern Ocean productivity by the irradiance-mixing regime. Limnology and Oceanography 36: 1650-1661

Oschlies A (2002) Nutrient supply to the surface waters of the North Atlantic: A model study. Journal of Geophysical Research: Oceans 107:14-13

Park J, Oh I-S, Kim H-C, Yoo S (2010) Variability of SeaWiFs Chlorophyll-a in the

1 southwest Atlantic sector of the Southern Ocean: Strong topographic effects and weak
2 seasonality. Deep-Sea Research Part I: Oceanographic Research Papers 57:604-620

3 Petrou K, Trimborn S, Rost B, Ralph P, Hassler C (2014) The impact of iron limitation on the
4 physiology of the Antarctic diatom Chaetoceros simplex. Marine Biology: 1-13

5 Priddle J, Smetacek V, Bathmann U, Stromberg J-O, Croxall JP (1992) Antarctic marine
6 primary production, biogeochemical carbon cycles and climatic change. Philosophical
7 Transactions of the Royal Society of London Series B: Biological Sciences 338:289-297

8 Sambrotto RN, Mace BJ (2000) Coupling of biological and physical regimes across the
9 Antarctic Polar Front as reflected by nitrogen production and recycling. Deep Sea Research
10 Part II: Topical Studies in Oceanography 47: 3339-3367

11 Schlitzer R (2002) Carbon export fluxes in the Southern Ocean: results from inverse modeling
12 and comparison with satellite based estimates. Deep-Sea Research II 49:1623-1644

13 Smetacek V, Assmy P, Henjes J (2004) The role of grazing in structuring Southern Ocean
14 pelagic ecosystems and biogeochemical cycles. Antarctic Science 16: 541-558

15 Smetacek V, et al. (2012) Deep carbon export from a Southern Ocean iron-fertilized diatom
16 bloom. Nature 487:313-319

17 Smith Jr WO, Marra J, Hiscock MR, Barber RT (2000) The seasonal cycle of phytoplankton
18 biomass and primary productivity in the Ross Sea, Antarctica. Deep-Sea Research Part II:
19 Topical Studies in Oceanography 47:3119-3140

20 Steinmetz F, Deschamps PY, Ramon D. (2011) Atmospheric correction in presence of sun
21 glint: application to MERIS. Optics express 19: 9783-9800

22 Strass, V.H. and Woods, J. D. (1991) New production in the summer revealed by the
23 meridional slope of the deep chlorophyll maximum. Deep-Sea Research, 38 (1), pp. 35-56

24 Strass VH, Naveira Garabato AC, Pollard RT, Fischer HI et al. (2002a) Mesoscale frontal
25 dynamics: Shaping the environment of primary production in the Antarctic Circumpolar
26 Current. Deep-Sea Research Part II: Topical Studies in Oceanography 49:3735-3769

27 Strass, VH, Naveira Garabato, AC, Bracher, AU, Pollard, RT, Lucas, MI (2002b): A 3-D
28 mesoscale map of primary production at the Antarctic Polar Front: results of a diagnostic
29 model. Deep-Sea Research Part II: Topical Studies in Oceanography 49: 3813

30 Strass, V.H. , Bathmann, U. , Rutgers v. d. Loeff, M. and Smetacek, V. (2002c): Mesoscale
31 physics, biogeochemistry and ecology of the Antarctic Polar Front, Atlantic Sector: An
32 Introduction to and summary of cruise ANT-XIII/2 of RV Polarstern. Deep-Sea Research
33 II: Topical Studies in Oceanography 49, pp. 3707-3711

34 Strass, VH, Leach, H, Prandke, H, Donnelly, M, Bracher, AU, Wolf-Gladrow, DA (in prep.)
35 The physical environmental conditions of biogeochemical differences along the ACC in the
36 Atlantic Sector during late austral summer 2012. This issue

37 Strickland JDH, Parsons TR (1968) A practical handbook of seawater analysis, Vol Bulletin.
38 No 167. Fisheries Research Board of Canada

39 Sunda WG, Huntsman SA (1997) Interrelated influence of iron, light and cell size on marine

phytoplankton growth. Nature 390:389-392

Tremblay JE, Lucas MI, Kattner G, Pollard R, Bathmann U, Strass V, Bracher A (2002) Significance of the Polar Frontal Zone for large-sized diatoms and new production during summer in the Atlantic Sector of the Southern Ocean. Deep-Sea Research II 49 18: 3793-3811

van Oijen T, van Leeuwe MA, Granum E, Weissing FJ, Bellerby RGJ, et al. (2004) Light rather than iron controls photosynthate production and allocation in Southern Ocean phytoplankton populations during austral autumn. Journal of Plankton Research 26: 885-900

Vaillancourt RD, Marra J, Barber RT, Smith Jr WO (2003) Primary productivity and in situ quantum yields in the Ross Sea and pacific sector of the Antarctic Circumpolar Current. Deep-Sea Research Part II: Topical Studies in Oceanography 50:559-578

Venables HJ, Meredith MP (2009) Theory and observations of Ekman flux in the chlorophyll distribution downstream of South Georgia. Geophysical Research Letters 36: GL23610

Veth C, Lancelot C, Ober S (1992) On processes determining the vertical stability of surface waters in the marginal ice zone of the north-western Weddell Sea and their relationship with phytoplankton bloom development. Polar Biol 12:237-243

Whitehouse MJ, Atkinson A, Korb RE, Venables HJ, Pond DW, Gordon M (2012) Substantial primary production in the land-remote region of the central and northern Scotia Sea. Deep-Sea Research Part II: Topical Studies in Oceanography 59–60:47-56

Whitehouse MJ, Korb RE, Atkinson A, Thorpe SE, Gordon M (2008) Formation, transport and decay of an intense phytoplankton bloom within the high-nutrient low-chlorophyll belt of the Southern Ocean. Journal of Marine Systems 70:150-167

Wolf-Gladrow D (2013) The expedition of the research vessel "Polarstern" to the Antarctic in 2012 (ANT-XXVIII/3). Berichte zur Polar- und Meeresforschung - Reports on Polar and Marine Research 661, Alfred Wegener Institute for Polar and Marine Research, Bremerhaven, 191 p.

Figure captions

Figure 1: Satellite-based Chl *a* maps - Mean Chl *a* concentrations (mg m^{-3}) during February 2012 derived from the satellite MERIS Polymer product. Stars indicate sampling locations during the ANT-XXVIII/3 cruise. Detailed view on the 39°W bloom north of South Georgia (B) and the 12°W bloom (C) with circles indicating station positions where Chl *a* concentrations were measured in-situ; red circle indicates the time-series station.

Figure 2: Average nutrient profiles – Concentrations of nitrate (A), phosphate (B) and silicate (C) in the top 500 m from the 12°W bloom (open symbols) and the 39°W bloom north of South Georgia (filled symbols).

Figure 3: Nutrient deficit ratios – Deficit ratios for $Si(OH)_4$:NO_3 versus NO_3:PO_4 [mol mol^{-1}] for all stations in the 12°W bloom (open symbols) and the 39°W bloom (filled symbols).

Figure 4: Relationships between NPP, MLD and Chl *a* – Depth-integrated net primary production versus mixed-layer depth (A), Chl *a* concentrations versus mixed-layer depth (B) and net primary production versus Chl *a* concentrations (C) for all stations in the 12°W bloom (open circles) and the 39°W bloom (filled circles) as well as the outstation (triangle). Lines indicate linear regression of all data.

Figure 5: Schematic overview - Similarities of and differences between the 39°W (A) and the 12°W bloom (B) in terms of MLDs, nutrient concentrations and deficits, NPP and pCO_2 as well as Chl *a* and zooplankton standing stocks.

Table 1: 100 m depth-integrated Chl *a* standing stocks [mg m^{-2}], primary productivity NPP [mg C m^{-2} d^{-1}], photosynthetic efficiency P^b [mg C (mg Chl *a*)$^{-1}$ d^{-1}], total PAR during on-deck incubations [mol photons m^{-2} d^{-1}]. Star symbol denotes central station in 12°W bloom.

Bloom area	Station #	Date	Longitude [°W]	Latitude [°S]	MLD [m]	Chl *a* [mg m^{-2}]	NPP [mg C m^{-2} d^{-1}]	P^b [mg C (mg Chl *a*)$^{-1}$ d^{-1}]	PAR [mol photons m^{-2} d^{-1}]
Outstation	PS79/085-03	26.01.12	8.00	52.00	30	9	161	17.6	14.45
12°W	PS79/086-02	29.01.12	11.99	52.00	87	180	2587	14.4	11.27
	PS79/091-05*	03.02.12	12.67	51.21	56	166	2816	17.0	16.40
	PS79/114-01*	08.02.12	12.67	51.20	78	143	2447	17.1	18.75
	PS79/128-10*	12.02.12	12.65	51.21	89	117	1669	14.2	13.80
	PS79/136-08*	14.02.12	12.66	51.20	55	85	1050	12.3	17.03
	PS79/137-07	15.02.12	12.17	51.04	84	136	1380	10.1	8.68
	PS79/138-02	15.02.12	12.49	51.11	65	88	1020	11.5	5.65
	PS79/139-03	15.02.12	12.99	51.00	57	52	796	15.4	6.01
	PS79/140-12*	17.02.12	12.66	51.19	68	115	1998	17.3	19.31
39°W	PS79/147-01	25.02.12	37.01	49.60	28	54	n.d.	n.d.	15.58
	PS79/149-01	25.02.12	36.98	48.80	12	25	573	22.7	13.17
	PS79/155-01	26.02.12	37.59	50.81	23	60.	769	12.8	5.28
	PS79/160-01	27.02.12	38.80	50.40	42	n.d.	640	n.d.	5.27
	PS79/165-05	28.02.12	39.40	49.60	40	89	1644	18.4	17.29
	PS79/168-01	29.02.12	38.76	48.80	43	73	1052	14.4	20.29
	PS79/169-01	29.02.12	38.80	49.20	44	39	786	20.3	19.06
	PS79/170-01	29.02.12	38.80	49.60	53	129	2220	16.1	19.61
	PS79/174-09	01.03.12	38.31	49.64	39	100	3023	30.3	17.76
	PS79/175-01	03.03.12	39.39	50.80	30	79	1575	20.0	19.49

Table 2: Comparison of phytoplankton biomass, productivity and POC:PON ratios as well as average 10-60 m nutrient concentrations, nutrient deficits and average deficit concentrations as well as deficit ratios for the two bloom areas investigated. Values denote average (± 1 s.d.)

Parameter	12°W bloom area		39°W bloom	
Chl *a* [mg Chl *a* m^{-2}]	120 ± 41	(n=9)	63 ±29	(n=9)
Net Primary Productivity [mg C m^{-2} d^{-1}]	1751 ± 747	(n=9)	1365 ±832	(n=10)
P^b [mg C (mg Chl *a*)$^{-1}$ d^{-1}]	14 ± 3	(n=9)	19 ±5	(n=8)
POC:PON [mol mol^{-1}]	4.6 ± 0.4	(n=25)	4.3 ±0.3	(n=24)
Chl *a*:POC [g:g]	32.7 ± 5.7	(n=8)	33.1 ±15.8	(n=5)
PAR [mol photons m^{-2} d^{-1}]	13 ± 5	(n=9)	15 ±6	(n=9)
MLD [m]	71 ± 14	(n=10)	35 ±13	(n=10)
NO_3 [mmol m^{-3}]	19.9 ± 0.5	(n=35)	16.3 ±1.8	(n=26)
PO_4 [mmol m^{-3}]	1.3 ± 0.1	(n=35)	1.2 ±0.1	(n=26)
$SiOH_4$ [mmol m^{-3}]	4.5 ± 3.1	(n=35)	2.2 ±1.3	(n=26)
NO_3 deficit concentration [mmol m^{-3}]	9.1 ±0.9	(n=35)	10.2 ±2.6	(n=26)
PO_4 deficit concentration [mmol m^{-3}]	0.6 ±0.1	(n=35)	0.6 ±0.2	(n=26)
$SiOH_4$ deficit concentration [mmol m^{-3}]	22.6 ±2.5	(n=35)	19.7 ±5.3	(n=26)
NO_3 deficit [mmol m^{-2}]	1087 ±108	(n=35)	1219 ±307	(n=26)
PO_4 deficit [mmol m^{-2}]	75 ± 7	(n=35)	68 ± 18	(n=26)
$SiOH_4$ deficit [mmol m^{-2}]	2712 ±303	(n=35)	2359 ± 631	(n=26)
NO_3:PO_4 deficit [mol mol^{-1}]	14.4 ± 0.9	(n=35)	17.9 ± 0.9	(n=26)
$SiOH_4$:NO_3 deficit [mol mol^{-1}]	2.5 ± 0.3	(n=35)	2.0 ± 0.4	(n=26)

Controls of primary production in two phytoplankton blooms in the Antarctic Circumpolar Current

Hoppe, C.J.M.[a]*, Klaas, C.[a], Ossebaar, S.[b], Soppa, M.A.[a], Cheah, W.[a,c], Laglera, L.M.[d], Santos-Echeandia, J.[e], Rost, B.[a], Wolf-Gladrow, D.A.[a], Bracher, A.[a,f], Hoppema, M.[a], Strass, V.[a], and Trimborn, S.[a,g]

[a]Alfred Wegener Institute - Helmholtz Centre for Polar and Marine Research, Am Handelshafen 12, 27570 Bremerhaven, Germany
[b]NIOZ - Royal Netherlands Institute for Sea Research, Landsdiep 4, 1797 SZ 't Horntje (Texel), The Netherlands
[c]Research Center for Environmental Changes, Academia Sinica, 128 Academia Road, 11529 Taipei, Taiwan
[d]FITRACE. Departamento de Química, Universidad de las Islas Baleares, Cra. de Valldemossa, Palma, Balearic Islands, 07122, Spain
[e]Marine Biogeochemistry, Instituto de Investigaciones marinas (CSIC), Eduardo Cabello 6, 36208, Vigo, Spain
[f]Institute of Environmental Physics, University Bremen, Otto Hahn Allee 1, 28359 Bremen, Germany
[g]Marine Botany, University Bremen, Leobener Straße NW2, 28359 Bremen, Germany

* Corresponding author (Clara.Hoppe@awi.de; +49 471 4831-2096)

Abstract

The Antarctic Circumpolar Current has a high potential for primary production and carbon sequestration through the biological pump. In the current study, two large-scale blooms observed in 2012 during a cruise with *RV* Polarstern were investigated with respect to phytoplankton standing stocks, primary productivity and nutrient budgets. While net primary productivity was similar in both blooms, chlorophyll *a* –specific photosynthesis was more efficient in the bloom closer to the island of South Georgia (39°W, 50°S) compared to the open ocean bloom further east (12°W, 51°S). We did not find evidence for light being the driver of bloom dynamics as chlorophyll standing stocks up to 165 mg m^{-2} developed despite mixed layers as deep as 90 m. Since the two bloom regions differ in their distance to shelf areas, potential sources of iron vary. Nutrient (nitrate, phosphate, silicate) deficits were similar in both areas despite different bloom ages, but their ratios indicated more pronounced iron limitation at 12°W compared to 39°W. While primarily the supply of iron and not the availability of light seemed to control onset and duration of the blooms, higher grazing pressure could have exerted a stronger control toward the declining phase of the blooms.

Keywords: biological pump; nutrient budgets; primary productivity; Southern Ocean

1. Introduction

Oceanic phytoplankton account for about half of the global primary production, thereby providing the basis of marine food webs and exerting a major control on biogeochemical cycles and global climate (Falkowski et al. 1998, Field et al. 1998). The supply of nutrients such as nitrate, phosphate and silicate to the photic zone (i.e. 'new' nutrients) constrains the biologically-mediated export of organic carbon to the deep ocean (Dugdale and Goering 1967, Eppley and Peterson 1979, Longhurst and Harrison 1989). The strength of this biological carbon pump can be estimated from the degree to which these nutrients are consumed as well as the carbon to nutrient ratios in the organic matter sinking to depth.

One area with great potential for an increase in both new and recycled production is the Antarctic Circumpolar Current (ACC). As concentrations of nitrate and phosphate are high, primary production is limited by other controlling factors (Priddle et al. 1992, Moore et al. 2000). More specifically, productivity in the ACC region is thought to be controlled by interactions between light availability (Mitchell and Holm-Hansen 1991, Nelson and Smith 1991), iron supply (Martin 1990, de Baar et al. 1995), silicate limitation (Brzezinski et al. 2003), and the effect of grazing (Dubischar and Bathmann 1997, Atkinson et al. 2001). More recent studies suggest that iron is the primary limiting factor in these open ocean areas (Smetacek et al. 2012). Phytoplankton blooms in the ACC tend to occur downstream of land masses and have been associated with fronts, islands and bathymetric features, which increase the input of iron and other trace metals into the surface waters (Moore et al. 1999, Blain et al. 2001, Borrione and Schlitzer 2013). In the Atlantic sector of the ACC, high phytoplankton standings stocks and production rates have been observed in the Antarctic Polar Frontal Zone (APFZ; Bathmann et al. 1997, Bracher et al. 1999, Moore and Abbott 2000, Tremblay et al. 2002). In this particular region, an alleviation of light limitation through upper water column stratification in spring was proposed as a trigger for the development of phytoplankton blooms. Finally, the termination of blooms is often caused by a combination of grazing pressure as well as iron and silicate limitation (Abbott et al. 2000, Tremblay et al. 2002).

Attempts to disentangle the effects of potential factors controlling bloom dynamics are complicated by the fact that these different factors tend to co-vary and also interact with each other (e.g. iron limitation decreases photoadaptive capabilities, thereby affecting light limitation; Sunda and Huntsman 1997, Petrou et al. 2014). The aim of the present study was, therefore, to understand how different environmental factors influence the biomass, primary productivity, nutrient usage and the potential for carbon sequestration in two large-scale phytoplankton blooms with a putatively different iron supply.

2. Material and methods

2.1. Cruise track and sampling locations

Sampling was conducted in the framework of the 'Eddy-Pump' project during the ANT-XXVIII/3 expedition on-board the German research vessel *Polarstern* (Wolf-Gladrow 2013) between January and March 2012 in two survey areas. In addition to physical properties, nutrient and chlorophyll concentrations as well as primary productivity were determined in two survey areas at 10 stations in a land-remote bloom at 50 - 52°S and 13.5 - 11.5°W (hereafter 12°W bloom) and at 9 stations in a bloom downstream of South Georgia at 48 - 52°S and 37 - 39°W (hereafter 39°W bloom; Figure 1). Water samples for all measured parameters except iron (see below), were obtained at discrete depths (10, 20, 40, 60, 80 and 100 m) from Niskin bottles attached to a Conductivity Temperature Depth (CTD) rosette. The mixed layer depth (MLD) was defined as a change of density of 0.02 kg m^{-3} relative to the uppermost value of each CTD vertical profile (Cisewski et al. 2005, Strass et al. this issue). It should be noted that at station PS79/085 (the out-station in the 12°W area), chlorophyll biomass was evenly distributed to a deeper pycnocline at a depth of 82 m even though the MLD determined was 30 m only.

2.2. Macronutrient measurements and nutrient deficit calculations

Macronutrients were measured colorimetrically using a Technicon TRAACS 800 auto-analyzer (Seal Analytical) on board the ship. Orthophosphate (PO_4^{3-}) was measured at 880 nm after the formation of molybdophosphate-complexes (Murphy and Riley 1962). Orthosilicate ($Si(OH)_4$) was measured at 820 nm after formation of silica-molybdenum complexes with oxalic acid being added to prevent the formation of phosphate-molybdenum (Strickland and Parsons 1968). After nitrate reduction through a copperized cadmium coil, nitrate plus nitrite ($NO_3^-+NO_2^-$) was measured at 550 nm after complexation with sulphanylamide and naphtylethylenediamine (Grasshoff et al. 1983). Complex formation without the reduction step was used to determine nitrite concentrations. Nitrate is calculated by subtracting the nitrite value from the 'NO_3+NO_2' value (Grasshoff et al. 1983).

Prior to analysis, all samples and standards were brought to 22°C in about 2 h. Concentrations were recorded in mmol m^{-3} at this temperature. Calibration standards were diluted from stock solutions of the different nutrients in 0.2 µm filtered low nutrient seawater. During every run, a freshly diluted mixed nutrient standard, containing silicate, phosphate and nitrate, the so-called 'NIOZ nutrient cocktail', was measured in triplicate. Every 2 weeks, a

sterilized 'Reference Material Nutrient Sample' (JRMNS, Kanso Technos, Japan) containing known concentrations of silicate, phosphate, nitrate and nitrite in Pacific Ocean water was analysed in triplicate. The cocktail and the JRMNS were both used to monitor the performance of the analyser. Finally, the NIOZ nutrient cocktail was used to adjust all data by multiplying with the offset factor derived from the differences between assigned and measured nutrient concentrations. The average standard deviations of the NIOZ nutrient cocktail measurements were 0.02 mmol m^{-3} for phosphate, 0.59 mmol m^{-3} for silicate and 0.13 mmol m^{-3} for nitrate (n=113).

Surface nutrient concentrations were calculated as the weighted average of the measured values for sampling depths 10 - 60 m, accounting for differences in sampling frequency with increasing depth. Nutrient deficits were calculated at each station as the differences between the nutrient concentration in remnant Antarctic Winter Water (AWW) in the layer below the seasonal pycnocline and the average concentrations above that (Jennings et al. 1984, Hoppema et al. 2000). The nutrient deficit per m^3 at each station was averaged over the different depths, while the deficit per m^2 was calculated by integrating the deficits from 10-120 m data for the water column of 0-120 m. It should be noted that nutrient deficits are suitable estimates for annual net community production only if vertical and lateral mixing in both the temperature minimum and the surface layer are small (Jennings et al. 1984, Hoppema et al. 2000, Hoppema et al. 2007). The deficits thus represent a somewhat larger area than just the station location. The AWW layer, which was characterised by a well-defined potential temperature minimum (Z_{tmin}) in the CTD profiles, was situated at 150 ± 15 m water depth during this cruise. AWW nutrient concentrations were similar in both bloom areas (2.1 ± 0.1 mmol m^{-3} for phosphate, 30.1 ± 6.1 mmol m^{-3} for silicate and 30.6 ± 1.4 mmol m^{-3} for nitrate; n=113; Figure 2). Deficit ratios (i.e. $Si(OH)_4$:NO_3 and NO_3:PO_4) were calculated after averaging the nutrient deficits from the different depths at each station.

2.3. Iron sampling and measurements

Samples for total dissolved iron (TDFe) measurements were collected from the upper 300 m of the water column in metal free GOFLO bottles attached to a Kevlar line. Samples were immediately online filtered through trace-metal clean 0.22 µm sterile capsules (Sartobran 300, Sartorius) and subsequently collected in low-density polyethylene bottles. TDFe was determined on-board by voltammetry following the protocol described by Laglera et al. (2013).

2.4. Irradiance estimates

Solar irradiance was measured continuously at one-minute intervals using a RAMSES hyperspectral radiometer (TriOS GmbH, Germany) placed on the uppermost deck of the ship to avoid shading. The sensor measured downwelling incident sunlight from 350 to 950 nm with a spectral resolution of 3.3 nm. Plane photosynthetically active radiation (PAR) was calculated as the integral of irradiances from 400 to 700 nm. Daily PAR values [mol photons m^{-2} d^{-1}] were then calculated by integrating the PAR values from the start to the end of each incubation (~24 h).

2.5. Chlorophyll a

Chlorophyll *a* (Chl *a*) concentrations were determined by two methods: fluorometry (Chl a_{FLUO}) and high performance liquid chromatography (HPLC; Chl a_{HPLC}). Except for stations PS79/160 and PS79/175, where Chl a_{FLUO} data were used, Chl *a* estimates are based on Chl a_{HPLC} data. The two Chl *a* datasets produced similar results, showing a significant correlation and only minimal differences ($r^2 = 0.97$, $p < 0.001$, n=104, Chl a_{FLUO} = 0.990* Chl a_{HPLC} + 0.0837).

For the Chl a_{FLUO} determination, samples were filtered onto 25 mm diameter GF/F filters (Whatman; 0.7 µm nominal pore size) at a vacuum of <100 mmHg. Filters were immediately transferred into centrifuge tubes containing 10 mL of 90% acetone and 1 cm^3 of glass beads. The tubes were sealed and stored at -20°C for at least 30 min and up to 24 h. Chl a_{FLUO} was extracted by placing the centrifuge tubes in a grinder for 3 min followed by centrifugation at 0°C. The supernatant was poured into quartz tubes and the Chl a_{FLUO} content was quantified in a 10-AU fluorometer (Turner). Calibration of the fluorometer was carried out at the beginning and at the end of the cruise, diverging by 2%. Chl a_{FLUO} content was calculated using the equation given in Knap et al. (1996) and the average parameter values from the two calibrations.

For the Chl a_{HPLC} determinations, samples were filtered onto 25 mm diameter GF/F filters (Whatman) at a vacuum of <100 mmHg. Filters were shock-frozen in liquid nitrogen and stored at -80°C until analysis in the home laboratory following the method described by Hoffmann et al. (2006) as detailed in Cheah et al. (this issue). For calculating Chl a_{HPLC} the sum of concentrations of monovinyl-, divinyl chlorophyll *a* and chlorophyllide *a* was taken (divinyl chlorophyll *a* was not detected in our samples).

Vertical plankton net samples were used to qualitatively determine the dominant phytoplankton functional types by means of light microscopy.

2.6. Particulate organic carbon and nitrogen

Samples for particulate organic carbon (POC) and nitrogen (PON) were filtered onto pre-combusted (15 h, 500°C) glass fibre filters (GF/F, Whatman). Filters were stored at -20°C and processed according to Lorrain et al. (2003). Analyses were performed using a CHNS-O elemental analyser (Euro EA 3000, HEKAtech).

2.7. Primary Productivity

Net primary production rates (NPP) were determined in duplicates by the incubation of 20 mL seawater sample spiked with 20 µCi $NaH^{14}CO_3$ (53.1 mCi $mmol^{-1}$; Perkin Elmer) in a 20 mL glass scintillation vial for 24 h in a seawater cooled on-deck incubator. Seawater samples from 6 depths (10, 20, 40, 60, 80 and 100 m) were incubated at different irradiances, which were achieved with neutral density filters decreasing incoming light to 25, 12.5, 6.3, 3.1, 1.6 and 0.8% of downwelling PAR above the ocean surface.

After the addition of the $NaH^{14}CO_3$ spike, 0.1 mL aliquots were immediately removed and mixed with 10 mL of scintillation cocktail (Ultima Gold AB, PerkinElmer). After 2 h, these samples were counted with a liquid scintillation counter (Tri-Carb 2900TR, PerkinElmer) to determine the total amount of added $NaH^{14}CO_3$ (100%). For blank determination, one additional replicate per sample was immediately acidified with 0.5 ml 6N HCl (blank). After the outdoor incubation of the samples over 24 h, ^{14}C incorporation was stopped by adding 0.5 mL 6N HCl to each vial. The vials were then left to degas overnight, thereafter 15 ml of scintillation cocktail (Ultima Gold AB) were added and samples were measured after 2 h with the same liquid scintillation counter. NPP rates [mg C m^{-3} d^{-1}] at each sample depth were calculated as follows:

$$NPP\ [mg\ C\ m^{-3}\ d^{-1}] = (DIC * (DPM_{sample} - DPM_{blank}) * 1.05) / (DPM_{100\%} * t) \quad (1)$$

where DIC is the concentration of dissolved inorganic carbon [µmol kg^{-1}], t is the incubation time [h] and 1.05 is the factor describing the discrimination between incorporation of ^{14}C and ^{12}C. DPM_{blank}, DPM_{sample} and $DPM_{100\%}$ are the disintegration per minute measured by the scintillation counter for the blank, the sample and the determination of the total amount of added $NaH^{14}CO_3$, respectively. Chl *a*-specific carbon fixation ($NPP_{Chl\ a}$ [mg C [mg Chl *a*]$^{-1}$ d^{-1}]) was calculated by dividing the depth-specific NPP value by the depth-specific Chl *a*

concentrations. Column-integrated $NPP_{Chl\ a}$ and primary productivity (NPP [mg C m^{-2} d^{-1}]) were derived by integrating values for 100 m depth.

2.8. Satellite Chl a maps

Weekly satellite maps of Chl *a* were used to study the development of the blooms. The comparison of satellite derived Chl *a* concentrations with the in-situ values measured at the two bloom locations was based on daily maps. The Chl *a* maps were derived using the POLYMER level-3 product of the Medium Resolution Imaging Spectrometer (MERIS) at a 0.02° spatial resolution (Steinmetz et al. 2011). POLYMER is an improved atmospheric correction algorithm for pixels contaminated by sun glint, thin clouds or heavy aerosol plumes. MERIS Polymer products improve the spatial coverage by almost a factor of two and have been proven successful for retrieving MERIS Ocean Colour products (Müller et al. 2015). The Chl *a* concentrations are retrieved using the standard OC4Me algorithm (Morel et al. 2007).

3. Results

3.1. Temporal and spatial development of the blooms

During austral summer (January - March) 2012, two large-scale phytoplankton blooms were observed in the APFZ (Figure 1A). A comparison of all surface Chl *a* concentrations (<10 m) derived by HPLC measurements with daily MERIS Polymer Chl *a* within the respective satellite pixel (Figure 1B, C) revealed a reasonable correlation coefficient ($r^2 = 0.67$), low bias (0.17 mg m^{-3}) and low percentage error (33%) between the two approaches. Estimates of Chl *a* standing stocks from in-situ measurements and satellite-based products are thus in good agreement, showing a nearly perfect match for the bloom situated at 12°W (Figure 1C). A reasonable agreement was observed for the 39°W bloom north of South Georgia, where satellite data tended to underestimate Chl *a* concentrations, particularly in the higher range of the measured values (Figure 1B). Both blooms were dominated by diatoms (C. Klaas, unpubl. results; also indicated by silicate depletion in the surface waters, Figure 2).

In the 12°W bloom area (Figure 1A, C), satellite Chl *a* maps indicated that a bloom developed from mid December 2011 onwards and peaked in the first two weeks of January 2012 with Chl *a* concentrations of around 3 mg m^{-3}. Our in-situ sampling took place between January 26th and February 15th, i.e. in the declining phase of the bloom. Within these three weeks, a central station (at 12°6'W, 51°2'S) was re-visited six times to investigate the temporal development of the bloom. The satellite data indicated that Chl *a* concentrations in the area quickly decreased within 5 days after the last sampling date to values lower than 1 mg m^{-3}.

The phytoplankton bloom at 39°W (Figure 1 A, B) was located in the Georgia Basin, north of the island of South Georgia. Satellite Chl *a* maps indicated that the 39°W bloom had already developed during mid-October and peaked in mid-December with surface Chl *a* concentrations reaching values higher than 3 mg m^{-3}. In-situ sampling took place between February 16th and March 3rd, in the declining phase of the bloom. Satellite data indicated that Chl *a* concentrations above 0.5 mg m^{-3} persisted at least until mid-March.

3.2. Phytoplankton standing stocks and primary productivity

In the 12°W area, average MLD was 71 ± 14 m. The depth-integrated Chl *a* concentrations in the bloom ranged from 50 to 180 mg Chl *a* m^{-2} (Table 1) and were on average 120 ±41 mg Chl *a* m^{-2}. Values were as low as 9 mg m^{-2} outside the bloom area (Table 2). NPP ranged from 800 to 2820 mg C m^{-2} d^{-1} (Table 1) and was on average 1750 ± 750 mg C m^{-2} d^{-1} (Table 2) in

the bloom, and thus significantly higher than values outside the bloom area (160 mg C m^{-2} d^{-1}). Chl *a*-specific carbon fixation $NPP_{Chl\ a}$, a measure of photosynthetic efficiency, varied between 10.1 and 17.3 mg C [mg Chl *a*]$^{-1}$ d^{-1} (on average 14.4 ± 2.6 mg C [mg Chl *a*]$^{-1}$ d^{-1}) in the 12°W bloom (Table 1 and 2). The average depth-integrated molar POC:PON ratios in this area were 6.3 ± 0.6 (Table 2). Average daily PAR during primary production measurements in the 12°W bloom was 12.3 ± 5.1 mol photons m^{-2} d^{-1} (Table 2).

In the 39°W bloom north of South Georgia, average MLD was 35 ± 13 m. In-situ Chl *a* standing stocks ranged from 25 to 130 mg Chl *a* m^{-2} (Table 1), with an average of 60 ± 30 mg Chl *a* m^{-2} (Table 2). NPP (Table 1) in this region varied between 570 and 3020 mg C m^{-2} d^{-1} (on average 1370 ± 830 mg C m^{-2} d^{-1}). $NPP_{Chl\ a}$ varied between 14.4 and 30.3 mg C [mg Chl *a*]$^{-1}$ d^{-1} (average of 19.4 ± 5.5 mg C [mg Chl *a*]$^{-1}$ d^{-1}). In the 39°W bloom, average depth-integrated molar POC:PON ratios (Table 2) were 5.9 ± 0.5. Average daily PAR during primary production measurements in this bloom was 15.7 ± 6.1 mol photons m^{-2} d^{-1} (Table 2).

Light profiles in the surface ocean were measured at 6 stations in the 12°W bloom area (with an average depth of the euphotic zone, Z_{eu} [0.8%], of 29.6 ±7.6 m) and only one station in the 39°W bloom area (Z_{eu} [0.8%] = 21.5 m), indicating similar euphotic depths in both blooms.

3.3. Nutrient concentrations and deficits

In the 12°W bloom area, average surface nutrient concentrations (10 m depth) were 19.7 ± 0.3 mmol NO_3 m^{-3}, 1.3 ± 0.1 mmol PO_4 m^{-3}, and 4.1 ± 3.1 mmol $Si(OH)_4$ m^{-3} (Figure 2). The average nutrient concentrations in the euphotic zone (10 - 60 m) were 20.6 ± 0.5 mmol NO_3 m^{-3}, 1.4 ± 0.1 mmol PO_4 m^{-3}, and 6.6 ± 2.7 mmol $Si(OH)_4$ m^{-3} (Table 2). Average integrated nutrient deficits in this area were 1090 ± 110 mmol NO_3 m^{-2}, 75 ± 7 mmol PO_4 m^{-2}, and 2710 ± 300 mmol $Si(OH)_4$ m^{-2} (Table 2) with a $Si(OH)_4$:NO_3 deficit ratio of 2.5 ± 0.3 mol mol^{-1} and a NO_3:PO_4 deficit ratio of 14 ± 1 mol mol^{-1} (Table 2, Figure 3). Average total dissolved iron (TDFe) concentrations in the upper 100m of the water column were 0.12 ± 0.03 nM (Table 2, Figure 4).

In the 39°W bloom area, average surface nutrient concentrations (10 m depth) were 14.9 ± 1.8 mmol NO_3 m^{-3}, 1.0 ± 0.1 mmol PO_4 m^{-3}, and 0.6 ± 0.5 mmol $Si(OH)_4$ m^{-3} (Figure 2). Average nutrient concentrations of the euphotic zone (10 - 60 m) were 16.3 ± 1.8 mmol NO_3 m^{-3}, 1.2 ± 0.1 mmol PO_4 m^{-3} and 2.2 ± 1.3 mmol $Si(OH)_4$ m^{-3} (Table 2). Resulting average integrated surface nutrient deficits in the 39°W bloom area were 1220 ± 310 mmol NO_3 m^{-2}, 68 ± 18 mmol PO_4 m^{-2} and 2360 ± 630 mmol $Si(OH)_4$ m^{-2} (Table 2), resulting in

$Si(OH)_4$:NO_3 deficit ratios of 2.0 ± 0.4 mmol $mmol^{-1}$ and NO_3:PO_4 deficit ratios of 17 ± 1 mmol $mmol^{-1}$ in this region (Table 2, Figure 3). 100 m averaged TDFe concentrations in this area were 0.14 ± 0.03 nM (Table 2, Figure 4).

Due to the high variability within each bloom, no significant differences in nutrient concentrations or deficits were detected between the two study areas (Table 2). The ratios of $Si(OH)_4$:NO_3 deficits, however, were significantly lower in the 39°W area compared to the 12°W bloom (t-test, $t = 6.6$, $p < 0.001$, $n = 35 + 26$; Table 2, Figure 3), while the ratios of NO_3:PO_4 deficits were significantly higher at 39°W (t-test, $t = 15.4$, $p < 0.001$, $n = 35 + 26$).

1 4. Discussion
2
3 *4.1. High variability of primary productivity in the APFZ*
4 Two large-scale diatom-dominated phytoplankton blooms in the Atlantic sector of the ACC
5 were observed (Figure 1), both being located between 50°S and 52°S in the Antarctic Polar
6 Frontal Zone (APFZ). Phytoplankton blooms are regularly observed in this region during
7 spring and summer (e.g. Laubscher et al. 1993, Bathmann et al. 1997, Bracher et al. 1999,
8 Tremblay et al. 2002). The occurrence of blooms in SO frontal zones has been associated with
9 oceanographic frontal features such as jet streams, meanders and mesoscale eddies, which can
10 lead to increased iron and silicate supply by mesoscale upwelling but also enhanced
11 stratification due to cross-frontal overlayering (de Jong et al. 1998, Bracher et al. 1999, Strass
12 et al. 2002a, Tremblay et al. 2002), thereby alleviating nutrient and light limitation for
13 phytoplankton growth. In the Georgia Basin, bloom initialization is thought to be mainly
14 driven by iron input from South Georgia, while further east more complex modes of iron
15 supply generate a larger degree of spatial and temporal variability in productivity (Venables
16 and Meredith 2009).
17 Being a relatively productive area within the otherwise HNLC (high-nutrient low-
18 chlorophyll) region, the APFZ has been the destination of several research cruises (e.g.
19 Bracher et al. 1999, Strass et al. 2002c, Tremblay et al. 2002, Korb and Whitehouse 2004).
20 Estimates of primary productivity in the APFZ vary between 100 and 6000 mg C m^{-2} d^{-1}
21 (Mitchell and Holm-Hansen 1991, Bracher et al. 1999, Moore and Abbott 2000, Strass et al.
22 2002b, Tremblay et al. 2002, Hiscock et al. 2003, Vaillancourt et al. 2003, Korb and
23 Whitehouse 2004, Park et al. 2010), with the highest values being observed in the vicinity of
24 land masses. The values observed in the present study are highly variable (about 160 - 3020
25 mg C m^{-2} d^{-1}; Table 1), but fall within the previously reported range. Antarctic phytoplankton
26 productivity in this region has been reported to exhibit strong spatial (Veth et al. 1992, Arrigo
27 et al. 1998), seasonal (Smith et al. 2000, Hiscock et al. 2003) and inter-annual variations
28 (Clarke and Leakey 1996, Park et al. 2010). Sporadic and patchy sampling during research
29 cruises makes it therefore difficult to estimate the specific productivity in this region. These
30 sampling opportunities are nonetheless useful to investigate the variability of productivity.
31 During sampling in the 12°W bloom, one station in the initial centre of the bloom was
32 investigated over a two-week period (Figure 1, Table 1). Primary productivity estimates at
33 this central sampling station varied between 1050 and 2820 mg C m^{-2} d^{-1} (Table 1). These
34 values are in the same range as reported by Jochem et al. (1995), but considerably higher than

previous estimates for this region (Bracher at al. 1999, Strass et al. 2002b, Tremblay et al. 2002, Korb and Whitehouse 2004). The observed temporal variability, which was somewhat lower than the spatial variability in the 12°W region (800 – 2820 mg C m^{-2} d^{-1}, Table 1), probably reflects a combination of the changes in light availability due to cloud cover (between 5 and 20 mol photons m^{-2} d^{-1}; Table 1) as well as the movement of water masses (Strass et al. this issue). The developmental phase of the phytoplankton bloom was also an important factor as primary production decreased over time (Table 1). During the investigation of the 39°W bloom, emphasis was put on the spatial variability in productivity (Figure 1, Table 1). In this bloom, primary productivity varied slightly more compared to the first area (570 - 3020 mg C m^{-2} d^{-1}; Table 1). This may be due to the higher spatial coverage, but also temporal aspects and the more dynamic currents play a role in this area (Strass et al. this issue). Nonetheless, even at three consecutive stations sampled on the same day (PS79/168-70) and within half a degree distance to each other, primary productivity varied between 790 and 2220 mg C m^{-2} d^{-1} (Table 1), demonstrating significant small-scale variability in the 39°W bloom area (Leach et al. this issue).

The high spatial and temporal variability emphasises once more the difficulties in estimating the productivity in this highly dynamic region (Abbott et al. 2000). Even though satellite Chl *a* estimates have drawbacks compared to in-situ measurements (Schlitzer 2002, Korb and Whitehouse 2004, Whitehouse et al. 2008), they provide higher spatial and temporal coverage of phytoplankton biomass at mesoscale resolution. The satellite Chl *a* from the MERIS Polymer-Chl-product used in this study has been validated globally and regionally within the current *ESA Climate Change Initiative for Ocean colour* and was chosen as the best algorithm for MERIS data processing (Müller et al. 2015). Also in the current study, the quality of the satellite Chl *a* data (r^2 = 0.67, bias = 0.17 mg m^{-3} compared to in-situ measurements) is sufficient to analyse the development of the two phytoplankton blooms at the surface. As satellite Chl *a* data only cover the ocean's first optical depth, estimates on primary productivity can only be derived using a model that incorporates satellite-based estimates of Chl *a*, sea surface temperature and PAR to reconstruct productivity over the entire mixed layer (e.g. Antoine and Morel 1996). Shipboard Chl *a* and primary productivity data are therefore necessary in order to verify the accuracy of satellite-derived products and to give information on the layers below the first optical depth. ^{14}C-based estimates tend to overestimate primary productivity due to the exclusion of loss terms such as sinking or grazing as well as biases in applied irradiances (e.g. Gall et al. 2001). Nonetheless, this

method can be used to investigate the underlying mechanisms for the patterns observed in satellite-derived maps.

4.2. Patterns in primary productivity do not correlate with MLDs

In the following, the two blooms are compared based on their general characteristics rather than investigating differences between single stations because relationships with the environmental conditions have to be considered on a wider scale, especially in such a highly dynamic region as the ACC.

In terms of depth-integrated primary productivity, no significant differences between the two blooms were observed during our visit (1750 ± 750 versus 1370 ± 830 mg C m^{-2} d^{-1}, t-test: t = 1.0, p = 0.315; Tables 1 and 2). Similar rates of primary productivity were achieved even though MLDs were significantly deeper in the 12°W compared to the 39°W bloom (71 ± 14 versus 35 ± 13 m, t-test: t = 6.0, p <0.001; Table 2). Hence, despite spending different proportions of the day in the deep low-light environment, phytoplankton communities of both blooms established similar primary productivity (Figure 5A; linear regression: r^2 = 0.208, p = 0.05). This finding is somewhat surprising, as earlier studies suggested that the alleviation from light limitation through shoaling MLDs is a key determinant of bloom development and productivity in the open SO (Sambrotto and Mace 2000, van Oijen et al. 2004, de Baar et al. 2005). In the current study, depth-integrated Chl *a* concentrations were positively correlated with MLD over the entire study area (Figure 5B). POC:Chl *a* ratios were similar in both blooms (Table 2), indicating that Chl *a* as well as biomass build-up was not light limited in MLDs up to 90 m (Figure 5A; linear regression: r^2 0.568, p = 0.0002). In fact, depth-integrated primary productivity was best correlated with depth-integrated Chl *a* concentrations (Figure 5C; linear regression: r^2 = 0.718, p < 0.0001). Hence, phytoplankton cells were overall able to acclimate to different light regimes and sustained similar depth-integrated primary productivity at different MLDs.

It should be kept in mind, however, that the controlling role of light may be particularly important early in the growing season when deep surface mixing occurs, light availability is limited, and phytoplankton biomass is low (Bracher et al. 1999, Franck et al. 2000, Smith et al. 2000, Landry et al. 2002, Llort et al. 2015). The effects of light might explain the earlier onset of the 39°W bloom (e.g. by stratification of the upper mixed layer), while the constant iron supply from South Georgia could have caused its longer duration. The light regime at the beginning of the growing season therefore may play an important role in modulating bloom dynamics by changing the rate and duration of biomass accumulation

during the build-up phase of the bloom. Even though primary productivity did not differ between blooms, the depth-integrated photosynthetic efficiencies derived from Chl *a*-specific carbon fixation ($NPP_{Chl\ a}$) were higher in the 39°W bloom compared to the 12°W bloom area (t-test, t = 2.5, p = 0.027). In the more deeply mixed 12°W bloom stations, lower $NPP_{Chl\ a}$-values indicate that phytoplankton photosynthesis was less efficient (Behrenfeld et al. 2008), possibly due to a combination of lower iron availability and deeper mixing regimes. Integrated over the water column, however, this did not lead to lower productivity than in the 39°W bloom.

4.3. Nutrient deficits indicate differences in iron availability over the growing season

During the growing season, phytoplankton take up and export nutrients to a certain degree as part of particulate organic matter, which can be expressed as nutrient deficits or depletions (Le Corre and Minas 1983, Jennings et al. 1984; Table 2). These proxies for net community production as well as their ratios differed between the two bloom areas (Figure 3). While the ratios of $Si(OH)_4$:NO_3 deficits were significantly higher in the 12°W compared to the 39°W bloom area (t-test, t = 6.6, p <0.001), the opposite trend was observed with respect to the NO_3:PO_4 deficit ratios (t-test: t = 15.4, p <0.001). As phytoplankton need iron for the assimilation of nitrate (and to a lesser degree of phosphate), the absence of iron leads to lowered uptake capacities (de Baar et al. 1997, Hutchins and Bruland 1998). While more generally, also taxonomic differences (e.g. diatom vs. flagellate dominated phytoplankton assemblages) affect nutrient deficit ratios, no such differences were observed in this study. And while shallow nitrification has been shown to influence SO nitrate concentrations in winter, it does not seem to influence nutrient concentrations and deficits in summer (Smart et al. 2015, cf. nitrate profiles in Figure 2). Our results therefore indicate differences in the nutrient assimilation histories of the two diatom-dominated phytoplankton assemblages, which is likely due to differences in magnitude and dynamics of iron supply in the two regions (i.e. higher iron input in the 39°W bloom area).

Drifter buoy trajectories indicate that water masses in the 39°W sampling region, which originate from the South Georgia shelf (Meredith et al. 2003) and most likely receives a higher and steadier supply of iron and other trace metals (Korb and Whitehouse 2004, Nielsdóttir et al. 2012, Borrione and Schlitzer 2013, Strass et al. this issue). In the area around 12°W, however, trace metal supply is thought to be restricted to deep-mixing during winter (Venables and Meredith, 2009), even though lateral transport could also play a role. During the time of sampling, iron measurements in the upper 100 m of the water column yielded

similarly low dissolved (0.1-0.2 µmol m^{-3}; Figure 5) and leachable particulate iron concentrations (0.2 - 0.8 µmol m^{-3}) in both areas (Table 2; Laglera et al. 2013, L. Laglera, unpubl. results), indicating iron depletion in both blooms. Given the development and intensity of the blooms as inferred from satellite data, iron concentrations must have been much higher at the onset of the blooms, yet they were already depleted by phytoplankton activity and particle scavenging at the time of sampling. Despite potentially large differences in iron availability and supply, surface silicate concentrations were similarly low in both areas and could potentially limit diatom growth (Figure 2; Nelson et al. 2001). Furthermore, nutrient deficits were also similar even though phytoplankton accumulation started earlier in the 39°W area (this study; Borrione and Schlitzer 2013). These similarities of the two blooms can partly be explained by the lower $Si(OH)_4$:NO_3 assimilation ratios at 39°W (Table 2), but may also suggest differences in the intensity of nutrient cycling, export and grazing pressure between the two systems.

4.4. From bottom-up towards top-down controls

Nutrient deficits can be used to estimate season-integrated net community production and are thus a proxy for new production on an annual basis (Jennings et al. 1984, Strass and Woods 1991, Hoppema et al. 2000, Whitehouse et al. 2012). Production rates calculated from nutrient deficits, however, can potentially be biased by altered nutrient concentrations due to vertical or lateral mixing and advection, alternative nutrient sources (e.g. ammonium), as well as changes in stoichiometry of organic matter (Jennings et al. 1984, Hoppema et al. 2007, Whitehouse et al. 2012). In agreement with Laubscher et al. (1993), slightly stronger nutrient depletion in the 39°W region co-occurred with higher photosynthetic efficiencies compared to 12°W (Table 2). This could indicate a better acclimation to their environment in the former bloom, potentially resulting from higher and steadier iron supply as well as easier photoacclimation in shallower mixed layers. The estimates of primary productivity and POC:PON as well as POC:Chl *a* ratios (Table 1 and 2), however, were in a similar range for both blooms. Furthermore, nutrient deficits, though somewhat lower in the 12°W bloom region, were not remarkably different between regions (Figure 3, Table 2). This is surprising, particularly in view of the almost two months earlier onset of the bloom in the Georgia Basin.

This apparent contradiction could have been caused by lower export efficiencies in the 39°W bloom. Shipboard carbonate chemistry measurements, however, revealed higher deficits in dissolved inorganic carbon (DIC) and a stronger CO_2 uptake from the atmosphere in the 39°W compared to the 12°W bloom area (Jones et al. this issue). Therefore, the

mismatch between nutrient deficits and bloom dynamics (as observed via satellites) was more likely caused by the highly dynamic currents in the 39°W area (Strass et al. this issue), which may have led to an underestimation of seasonal nutrient deficits due to higher lateral nutrient input (Oschlies 2002). Furthermore, net productivity may have been overestimated to different degrees in both blooms because loss terms such as grazing tend to be underestimated in ^{14}C-based measurements (e.g. Gall et al. 2001).

Recent field-, satellite- and model-based studies have highlighted the thus-far underestimated importance of top-down control mechanisms for phytoplankton bloom dynamics (e.g. Behrenfeld and Boss 2014, Llort et al. 2015). As the average zooplankton biomass in the South Georgia area is larger than anywhere else in the Southern Ocean (Atkinson et al. 2001), we speculate that during the time of sampling, top-down control was more strongly developed in the 39°W compared to the 12°W bloom area. Zooplankton sampling during our cruise showed that, despite high spatial variability, the zooplankton community around 39°W was in a more progressed state of development compared to the 12°W bloom area. In the latter, the proportion of small organisms and early developmental stages was higher (E. Pakomov and B. Hunt, unpubl. data). A potentially lower grazing pressure in the 12°W bloom could also be explained by a lower probability for predator-prey encounters in deeper MLDs (Behrenfeld 2010). In fact, this dilution effect on grazing rates might have contributed to the positive correlation between biomass and MLD found throughout our study (Figure 5B).

As the control of phytoplankton bloom dynamics in the ACC can shift from bottom-up to mainly top-down within a few weeks (Abbott et al. 2000, Llort et al. 2015), also a slightly earlier bloom development at 39°W could have led to our observations. Diatom-dominated blooms, as observed in this study (C. Klaas, unpubl. results), are mainly grazed by larger zooplankton. One can therefore assume that the usual time lag between bloom and grazer development (Smetacek et al. 2004) was still allowing phytoplankton biomass build-up in the 12°W area, while grazers already imposed a strong control on the 39°W bloom during the time of sampling. Satellite Chl *a* maps of the two bloom areas indeed show that the 39°W bloom developed around 8 weeks earlier than the 12°W bloom. We thus conclude that, despite both being in the apex phase, we visited the two areas at different stages of the bloom development.

5. Conclusions and biogeochemical implications

The results of this study suggest that a combination of different drivers strongly affect primary productivity in the SO. Bottom-up processes control the rate of build-up of a bloom, while top-down processes seem to be more important for determining the phytoplankton standing stock at the late bloom stage, i.e. when sampling took place (Figure 6). In contrast to earlier suggestions (van Oijen et al. 2004, de Baar et al. 2005), we did not observe significant light limitation of phytoplankton communities in two highly productive open-ocean areas of the Atlantic sector of the SO. Our results indeed indicate that, despite MLDs being deeper than 90 m, this does not necessarily prevent the development of phytoplankton blooms in the APFZ. Instead, iron supply seems to be the bottom-up process playing a pivotal role, particularly for determining bloom development and its potential duration, but also by modulating the light-use efficiency of phytoplankton (Smetacek et al. 2012, Behrenfeld and Milligan 2013). Considering the time scales of the individual measurements, we were thus able to explain the observed patterns by differences in iron availability and grazing pressure.

Acknowledgements

We would like to thank all scientists as well as the captain, officers and crew of RV *Polarstern* for their work and support during the ANT-XXVIII/3 cruise. Especially, we would like to thank E. Jones and M. Iversen for helpful discussions on the present dataset. We thank S. Wiegmann for help with the HPLC analysis, F. Steinmetz (HYGEOS) for supplying Polymer-MERIS CHL data and ESA for MERIS level-1 satellite data. We also thank E. Jones for providing DIC measurements. Furthermore, we would like to thank F. Altvater, D. Kottmeier, R. Kottmeier, T. Rueger, V. Schourup-Kristensen for their help during the cruise as well as A. Terbrüggen, K.-U. Richter and U. Richter for help with the cruise preparations. C.J.M.H. and B.R. were funded by the European Research Council (ERC) under the European Community's Seventh Framework Programme (FP7 / 2007-2013), ERC grant agreement no. 205150. S.T. was funded by the German Science Foundation (DFG), project TR 899/2 and the Helmholtz Impulse Fond (HGF Young Investigator Group EcoTrace). Funding to M.S. was supplied by CAPES, Brazil, and to A.B. by the Helmholtz Innovation Fund Phytooptics. This work was funded by the MINECO of Spain (Grant CGL2010-11846-E) and the Government of the Balearic Islands (Grant AAEE083/09). J.S.E. was supported by the JAE-Doc program of the CSIC. M.H. was supported through EU FP7 project CARBOCHANGE, which received funding from the European Community's Seventh Framework Programme under grant agreement no. 264879. This work was furthermore supported by the DFG in the framework of the priority programme "Antarctic Research with comparative investigations in Arctic ice areas" by a grant HO 4680/1.

References

Abbott MR, Richman JG, Letelier RM, Bartlett JS (2000) The spring bloom in the Antarctic polar frontal zone as observed from a mesoscale array of bio-optical sensors. Deep-Sea Research Part II: Topical Studies in Oceanography 47:3285-3314

Antoine D, Morel A (1996). Oceanic primary production: I. Adaptation of a spectral light-photosynthesis model in view of application to satellite chlorophyll observations, Global Biogeochemical Cycles 10:43-55

Arrigo KR, Worthen D, Schnell A, Lizotte MP (1998) Primary production in Southern Ocean waters. Journal of Geophysical Research: Oceans 103:15587-15600

Atkinson A, Whitehouse MJ, Priddle J, Cripps GC, Ward P, Brandon MA (2001) South Georgia, Antarctica: A productive, cold water, pelagic ecosystem. Marine Ecology Progress Series 216:279-308

Bathmann UV, Scharek R, Klaas C, Dubischar CD, Smetacek V (1997) Spring development of phytoplankton biomass and composition in major water masses of the Atlantic sector of the Southern Ocean. Deep-Sea Research Part II: Topical Studies in Oceanography 44:51-67

Behrenfeld MJ (2010) Abandoning Sverdrup's Critical Depth Hypothesis on phytoplankton blooms. Ecology 91: 977-989

Behrenfeld MJ, Halsey KH, Milligan AJ (2008) Evolved physiological responses of phytoplankton to their integrated growth environment. Philosophical Transactions of the Royal Society B: Biological Sciences 363:2687-2703

Behrenfeld MJ, Milligan AJ (2013) Photophysiological Expressions of Iron Stress in Phytoplankton. Annual Review of Marine Science 5: 217-246

Behrenfeld MJ, Boss ES (2014) Resurrecting the ecological underpinnings of ocean plankton blooms. Annual Review of Marine Science 6: 167-194

Blain S, Tréguer P, Belviso S, Bucciarelli E et al. (2001) A biogeochemical study of the island mass effect in the context of the iron hypothesis: Kerguelen islands, Southern Ocean. Deep-Sea Research Part I: Oceanographic Research Papers 48:163-187

Borrione, I, Schlitzer R (2013) Distribution and recurrence of phytoplankton blooms around South Georgia, Southern Ocean. Biogeosciences 10:217-231

Boyd PW (2002) Environmental factors controlling phytoplankton processes in the Southern Ocean. Journal of Phycology 38:844-861

Boyd PW, Ellwood MJ (2010) The biogeochemical cycle of iron in the ocean. Nature Geoscience 3:675-682

Bracher AU, Kroon BMA, Lucas MI (1999) Primary production, physiological state and composition of phytoplankton in the Atlantic sector of the Southern Ocean. Marine Ecology Progress Series 190: 1-16

Brzezinski MA, Dickson M-L, Nelson DM, Sambrotto R (2003) Ratios of Si, C and C uptake by microplankton in the Southern Ocean. Deep-Sea Research Part II: Topical Studies in Oceanography 50:619-633

Buesseler KO, Boyd PW (2009) Shedding light on processes that control particle export and flux attenuation in the twilight zone of the open ocean. Limnology and Oceanography 54: 1210-1232

Cheah W, et al. (submitted) Importance of silicic acid in regulating phytoplankton biomass and community structure in the iron-limited Antarctic Polar Front, this issue.

Cisewski B, Strass VH, Prandke H (2005) Upper-ocean vertical mixing in the Antarctic Polar Front Zone. Deep Sea Research Part II: Topical Studies in Oceanography 52:1087-1108

Clarke A, Leakey RJ (1996) The seasonal cycle of phytoplankton, macronutrients, and the microbial community in a nearshore antarctic marine ecosystem. Limnology and Oceanography 41:1281-1294

Coale, KH, et al. (2004) Southern Ocean Iron Enrichment Experiment: Carbon cycling in high- and low-Si waters. Science 304:408-414

de Baar H, Boyd P, Coale K, Landry M, Tsuda A et al. (2005) Synthesis of iron fertilization experiments: From the iron age in the age of enlightenment. J Geophys Res Oceans 110: C09S16

de Baar HJW, de Jong JTM, Bakker DCE, Loscher BM, Veth C, Bathmann U, V. Smetacek V (1995) Importance of iron for plankton blooms and carbon dioxide drawdown in the Southern Ocean. Nature 373:412-415

de Baar HJW, Van Leeuwe MA, Scharek R, Goeyens L, Bakker KMJ, Fritsche P(1997) Nutrient anomalies in *Fragilariopsis kerguelensis* blooms, iron deficiency and the nitrate/phosphate ratio (A. C. Redfield) of the Antarctic Ocean. Deep-Sea Research Part II: Topical Studies in Oceanography 44:229-260

de Jong JTM, den Das J, Bathmann U, Stoll MHC, Kattner G, Nolting RF, de Baar HJW (1998) Dissolved iron at subnanomolar levels in the Southern Ocean as determined by ship-board analysis. Analytica Chimica Acta 377:113-124

Dubischar CD, Bathmann UV (1997) Grazing impact of copepods and salps on phytoplankton in the Atlantic sector of the Southern Ocean. Deep-Sea Research Part II: Topical Studies in Oceanography 44:415-433

Dugdale RC, Goering JJ (1967) Uptake of new and regenerated forms of nitrogen in primary productivity. Limnology and Oceanography 12:196–206

Eppley RW, Peterson BJ (1979) Particulate organic matter flux and planktonic new production in the deep ocean. Nature 282: 677-680

Falkowski PG, Barber RT, Smetacek V (1998) Biogeochemical controls and feedbacks on ocean primary production. Science 281:200-206

Field CB, Behrenfeld MJ, Randerson JT, Falkowski P (1998) Primary production of the biosphere: Integrating terrestrial and oceanic components. Science 281:237-240

Gall MP, Strzepek R, Maldonado M, Boyd PW (2001) Phytoplankton processes. Part 2: Rates of primary production and factors controlling algal growth during the Southern Ocean iron release experiment (soiree). Deep-Sea Research Part II: Topical Studies in Oceanography

48:2571-2590

Grasshoff K, Kremling K, Ehrhardt M (1999) Methods of Seawater Analysis, Weinheim, Wiley-VCH

Hiscock MR, Marra J, Smith WO, Goericke R et al. (2003) Primary productivity and its regulation in the pacific sector of the Southern Ocean. Deep-Sea Research II 50:533-558

Hoffmann LJ, Peeken I, Lochte K, Assmy P, Veldhuis M (2006) Different reactions of Southern Ocean phytoplankton size classes to iron fertilization, Limnology andOceanography 51: 1217-1229

Hoppema M, Goeyens L, Fahrbach E (2000) Intense nutrient removal in the remote area off Larsen Ice Shelf (Weddell Sea). Polar Biology 23:85-94

Hoppema M, Middag R, de Baar HJW, Fahrbach E, van Weerlee EM, Thomas H (2007) Whole season net community production in the Weddell Sea. Polar Biology 31:101-111

Hutchins D, Bruland K (1998) Iron-limited diatom growth and Si:N uptake ratios in a coastal upwelling regime. Nature 393:561

Jennings JC, Gordon LI, Nelson DM (1984) Nutrient depletion indicates high primary productivity in the Weddell Sea. Nature 309:51-54

Jochem F, Mathot S, Quéguiner B (1995) Size-fractionated primary production in the open Southern Ocean in austral spring. Polar Biology 15: 381-392

Jones EM, Hoppema M, Strass V, Hauck J, Salt L, Klaas C, van Heuven SMAC, Wolf-Gladrow D, de Baar HJW (submitted): Mesoscale features create hotspots of carbon uptake in the Antarctic Circumpolar Current. This issue

Knap A, Michaels A, Close HD, Dickson A (1996) Protocols for the joint global ocean flux study (JGOFS) core measurements. UNESCO

Korb RE, Whitehouse M (2004) Contrasting primary production regimes around South Georgia, Southern Ocean: Large blooms versus high nutrient, low chlorophyll waters. Deep-Sea Research Part I: Oceanographic Research Papers 51:721-738

Laglera LM, Santos-Echeandía J, Caprara S, Monticelli D (2013) Quantification of Iron in Seawater at the Low Picomolar Range Based on Optimization of Bromate/Ammonia/ Dihydroxynaphtalene System by Catalytic Adsorptive Cathodic Stripping Voltammetry. Analytical Chemistry 85:2486-2492

Landry MR, Selph KE, Brown SL, Abbott MR et al. (2002) Seasonal dynamics of phytoplankton in the Antarctic polar front region at 170 °W. Deep-Sea Research Part II: Topical Studies in Oceanography 49:1843-1865

Leach, H, Strass, V, Prandke, H (submitted) Mixing and Finescale Structures in two Mesoscale Features of the Antarctic Circumpolar Current. This issue

Laubscher RK, Perissinotto R, McQuaid CD (1993) Phytoplankton production and biomass at frontal zones in the Atlantic sector of the Southern Ocean. Polar Biology 13:471-481

Le Corre P, Minas HJ (1983) Distributions et évolution des éléments nutritifs dans le secteur indien de l'Océan Antarctique en fin de période estivale. Oceanologica Acta 6:365-381

Llort J, Lévy M, Sallée J-B, Tagliabue A (2015) Onset, intensification, and decline of phytoplankton blooms in the Southern Ocean. ICES Journal of Marine Science: Journal du Conseil (in press)

Longhurst AR, Glen Harrison W (1989) The biological pump: Profiles of plankton production and consumption in the upper ocean. Progress in Oceanography 22:47-123

Lorrain A, Savoye N, Chauvaud L, Paulet Y-M, Naulet N (2003) Decarbonation and preservation method for the analysis of organic C and N contents and stable isotope ratios of low-carbonated suspended particulate material. Analytica Chimica Acta 491:125-133

Martin JH (1990) Glacial-interglacial CO_2 change: The iron hypothesis. Paleoceanography 5:1-13

Meredith MP, Watkins JL, Murphy EJ, Cunningham NJ et al. (2003) An anticyclonic circulation above the northwest Georgia Rise, Southern Ocean. Geophysical Research Letters 30:GL018039

Mitchell BG, Holm-Hansen O (1991) Observations and modeling of the Antarctic phytoplankton crop in relation to mixing depth. Deep-Sea Research 38:981-1007

Moore JK, Abbott MR (2000) Phytoplankton chlorophyll distributions and primary production in the southern ocean. Journal of Geophysical Research: Oceans 105:28709-28722

Moore JK, Abbott MR, Richman JG, Nelson DM (2000) The Southern Ocean at the last glacial maximum: A strong sink for atmospheric carbon dioxide. Global Biogeochem Cycles 14:455-475

Moore JK, Abbott MR, Richman JG, Smith WO et al. (1999) SeaWiFs satellite ocean color data from the Southern Ocean. Geophysical Research Letters 26:1465-1468

Morel A, Huot Y, Gentili B, Werdell PJ, Hooker SB, Franz BA (2007) Examining the consistency of products derived from various ocean color sensors in open ocean (Case 1) waters in the perspective of a multi-sensor approach. Remote Sensing of Environment 111: 69-88

Müller D, Krasemann H, Brewin RJW, Brockmann C, Deschams P-Y, et al. (2015) The Ocean Colour Climate Change Initiative: II. Spatial and temporal homogeneity of satellite data retrieval due to systematic effects in atmospheric correction processors. Remote Sensing of Environment (in press)

Murphy J, Riley JP (1962) A modified single solution method for the determination of phosphate in natural waters. Analytica Chimica Acta 27:31-36

Nelson DM, Brzezinski MA, Sigmon DE, Franck VM (2001) A seasonal progression of Si limitation in the pacific sector of the Southern Ocean. Deep-Sea Research Part II: Topical Studies in Oceanography 48:3973-3995

Nelson DM, Smith WOJ (1991) Sverdrup revisited: Critical depths, maximum chlorophyll levels, and the control of Southern Ocean productivity by the irradiance-mixing regime. Limnology and Oceanography 36: 1650-1661

Oschlies A (2002) Nutrient supply to the surface waters of the North Atlantic: A model study.

Journal of Geophysical Research: Oceans 107:14-13

Park J, Oh I-S, Kim H-C, Yoo S (2010) Variability of SeaWiFs Chlorophyll-a in the southwest Atlantic sector of the Southern Ocean: Strong topographic effects and weak seasonality. Deep-Sea Research Part I: Oceanographic Research Papers 57:604-620

Petrou K, Trimborn S, Rost B, Ralph P, Hassler C (2014) The impact of iron limitation on the physiology of the Antarctic diatom Chaetoceros simplex. Marine Biology: 1-13

Priddle J, Smetacek V, Bathmann U, Stromberg J-O, Croxall JP (1992) Antarctic marine primary production, biogeochemical carbon cycles and climatic change. Philosophical Transactions of the Royal Society of London Series B: Biological Sciences 338:289-297

Sambrotto RN, Mace BJ (2000) Coupling of biological and physical regimes across the Antarctic Polar Front as reflected by nitrogen production and recycling. Deep Sea Research Part II: Topical Studies in Oceanography 47: 3339-3367

Schlitzer R (2002) Carbon export fluxes in the Southern Ocean: results from inverse modeling and comparison with satellite based estimates. Deep-Sea Research II 49:1623-1644

Smart SM, Fawcett SE, Thomalla SJ, Weigand MA, Reason CJC, et al. (2015) Isotopic evidence for nitrification in the Antarctic winter mixed layer. Global Biogeochemical Cycles 29: 427-445

Smetacek V, Assmy P, Henjes J (2004) The role of grazing in structuring Southern Ocean pelagic ecosystems and biogeochemical cycles. Antarctic Science 16: 541-558

Smetacek V, et al. (2012) Deep carbon export from a Southern Ocean iron-fertilized diatom bloom. Nature 487:313-319

Smith Jr WO, Marra J, Hiscock MR, Barber RT (2000) The seasonal cycle of phytoplankton biomass and primary productivity in the Ross Sea, Antarctica. Deep-Sea Research Part II: Topical Studies in Oceanography 47:3119-3140

Steinmetz F, Deschamps PY, Ramon D. (2011) Atmospheric correction in presence of sun glint: application to MERIS. Optics express 19: 9783-9800

Strass, V.H. and Woods, J. D. (1991) New production in the summer revealed by the meridional slope of the deep chlorophyll maximum. Deep-Sea Research, 38 (1), pp. 35-56

Strass VH, Naveira Garabato AC, Pollard RT, Fischer HI et al. (2002a) Mesoscale frontal dynamics: Shaping the environment of primary production in the Antarctic Circumpolar Current. Deep-Sea Research Part II: Topical Studies in Oceanography 49:3735-3769

Strass, VH, Naveira Garabato, AC, Bracher, AU, Pollard, RT, Lucas, MI (2002b): A 3-D mesoscale map of primary production at the Antarctic Polar Front: results of a diagnostic model. Deep-Sea Research Part II: Topical Studies in Oceanography 49: 3813

Strass, V.H. , Bathmann, U. , Rutgers v. d. Loeff, M. and Smetacek, V. (2002c): Mesoscale physics, biogeochemistry and ecology of the Antarctic Polar Front, Atlantic Sector: An Introduction to and summary of cruise ANT-XIII/2 of RV Polarstern. Deep-Sea Research II: Topical Studies in Oceanography 49, pp. 3707-3711

Strass, VH, Leach, H, Prandke, H, Donnelly, M, Bracher, AU, Wolf-Gladrow, DA

(submitted) The physical environmental conditions of biogeochemical differences along the ACC in the Atlantic Sector during late austral summer 2012. This issue

Strickland JDH, Parsons TR (1968) A practical handbook of seawater analysis, Vol Bulletin. No 167. Fisheries Research Board of Canada

Sunda WG, Huntsman SA (1997) Interrelated influence of iron, light and cell size on marine phytoplankton growth. Nature 390:389-392

Tremblay JE, Lucas MI, Kattner G, Pollard R, Bathmann U, Strass V, Bracher A (2002) Significance of the Polar Frontal Zone for large-sized diatoms and new production during summer in the Atlantic Sector of the Southern Ocean. Deep-Sea Research II 49 18: 3793-3811

van Oijen T, van Leeuwe MA, Granum E, Weissing FJ, Bellerby RGJ, et al. (2004) Light rather than iron controls photosynthate production and allocation in Southern Ocean phytoplankton populations during austral autumn. Journal of Plankton Research 26: 885-900

Vaillancourt RD, Marra J, Barber RT, Smith Jr WO (2003) Primary productivity and in situ quantum yields in the Ross Sea and pacific sector of the Antarctic Circumpolar Current. Deep-Sea Research Part II: Topical Studies in Oceanography 50:559-578

Venables HJ, Meredith MP (2009) Theory and observations of Ekman flux in the chlorophyll distribution downstream of South Georgia. Geophysical Research Letters 36: GL23610

Veth C, Lancelot C, Ober S (1992) On processes determining the vertical stability of surface waters in the marginal ice zone of the north-western Weddell Sea and their relationship with phytoplankton bloom development. Polar Biol 12:237-243

Whitehouse MJ, Atkinson A, Korb RE, Venables HJ, Pond DW, Gordon M (2012) Substantial primary production in the land-remote region of the central and northern Scotia Sea. Deep-Sea Research Part II: Topical Studies in Oceanography 59–60:47-56

Whitehouse MJ, Korb RE, Atkinson A, Thorpe SE, Gordon M (2008) Formation, transport and decay of an intense phytoplankton bloom within the high-nutrient low-chlorophyll belt of the Southern Ocean. Journal of Marine Systems 70:150-167

Wolf-Gladrow D (2013) The expedition of the research vessel "Polarstern" to the Antarctic in 2012 (ANT-XXVIII/3). Berichte zur Polar- und Meeresforschung - Reports on Polar and Marine Research 661, Alfred Wegener Institute for Polar and Marine Research, Bremerhaven, 191 p.

Figure captions

Figure 1: Satellite-based Chl *a* maps - Mean Chl *a* concentrations (mg m^{-3}) during February 2012 derived from the satellite MERIS Polymer product. Stars indicate sampling locations during the ANT-XXVIII/3 cruise. Detailed view on the 39°W bloom north of South Georgia (B) and the 12°W bloom (C) with circles indicating station positions where Chl *a* concentrations were measured in-situ; red circle indicates the time-series station.

Figure 2: Average nutrient profiles – Concentrations of nitrate (A), nitrite (B), phosphate (C) and silicate (D) in the top 500 m from the 12°W bloom (open symbols) and the 39°W bloom north of South Georgia (filled symbols).

Figure 3: Nutrient deficit ratios – Deficit ratios for $Si(OH)_4$:NO_3 versus NO_3:PO_4 [mol mol^{-1}] for all stations in the 12°W bloom (open symbols) and the 39°W bloom (filled symbols).

Figure 4: Average total dissolved iron (TDFe) profiles for all stations sampled in the 12°W bloom (n=8; open symbols) and the 39°W bloom (n=2; filled symbols).

Figure 5: Relationships between net primary production, mixed layer depth and Chl *a* – Depth-integrated NPP versus MLD (A), Chl *a* concentrations versus MLD (B) and NPP versus Chl *a* concentrations (C) for all stations in the 12°W bloom (open circles) and the 39°W bloom (filled circles) as well as the outstation (triangle). Lines indicate linear regression of all data.

Figure 6: Schematic overview - Similarities of and differences between the 39°W (A) and the 12°W bloom (B) in terms of MLDs, nutrient concentrations and deficits, NPP and pCO_2 as well as Chl *a* and zooplankton standing stocks.

Table 1: 100 m depth-integrated Chl *a* standing stocks [mg m^{-2}], primary productivity NPP [mg C m^{-2} d^{-1}], photosynthetic efficiency $NPP_{Chl\ a}$ [mg C (mg Chl *a*)$^{-1}$ d^{-1}], total PAR during on-deck incubations [mol photons m^{-2} d^{-1}]. Star symbol denotes central station in 12°W bloom.

Bloom area	Station #	Date	Longitude [°W]	Latitude [°S]	MLD [m]	Chl *a* [mg m^{-2}]	PAR [mol photons m^{-2} d^{-1}]	NPP [mg C m^{-2} d^{-1}]	$NPP_{Chl\ a}$ [mg C (mg Chl *a*)$^{-1}$ d^{-1}]
Outstation	PS79/085-03	26.01.12	8.00	52.00	30	9	14.45	161	17.6
12°W	PS79/086-02	29.01.12	11.99	52.00	87	180	11.27	2587	14.4
	PS79/091-05*	03.02.12	12.67	51.21	56	166	16.40	2816	17.0
	PS79/114-01*	08.02.12	12.67	51.20	78	143	18.75	2447	17.1
	PS79/128-10*	12.02.12	12.65	51.21	89	117	13.80	1669	14.2
	PS79/136-08*	14.02.12	12.66	51.20	55	85	17.03	1050	12.3
	PS79/137-07	15.02.12	12.17	51.04	84	136	8.68	1380	10.1
	PS79/138-02	15.02.12	12.49	51.11	65	88	5.65	1020	11.5
	PS79/139-03	15.02.12	12.99	51.00	57	52	6.01	796	15.4
	PS79/140-12*	17.02.12	12.66	51.19	68	115	19.31	1998	17.3
39°W	PS79/147-01	25.02.12	37.01	49.60	28	54	15.58	n.d.	n.d.
	PS79/149-01	25.02.12	36.98	48.80	12	25	13.17	573	22.7
	PS79/155-01	26.02.12	37.59	50.81	23	60.	5.28	769	12.8
	PS79/160-01	27.02.12	38.80	50.40	42	n.d.	5.27	640	n.d.
	PS79/165-05	28.02.12	39.40	49.60	40	89	17.29	1644	18.4
	PS79/168-01	29.02.12	38.76	48.80	43	73	20.29	1052	14.4
	PS79/169-01	29.02.12	38.80	49.20	44	39	19.06	786	20.3
	PS79/170-01	29.02.12	38.80	49.60	53	129	19.61	2220	16.1
	PS79/174-09	01.03.12	38.31	49.64	39	100	17.76	3023	30.3
	PS79/175-01	03.03.12	39.39	50.80	30	79	19.49	1575	20.0

Table 2: Comparison of phytoplankton biomass, productivity and POC:PON ratios as well as average 10-60 m nutrient concentrations, nutrient deficits and average deficit concentrations as well as deficit ratios and 100 m depth-averaged TDFe concentrations for the two bloom areas investigated. Values denote average (± 1 s.d.).

Parameter	12°W bloom area		39°W bloom	
Chl *a* [mg Chl *a* m^{-2}]	120 ± 41	(n=9)	63 ±29	(n=9)
Net Primary Productivity [mg C m^{-2} d^{-1}]	1751 ± 747	(n=9)	1365 ±832	(n=10)
$NPP_{Chl\ a}$ [mg C (mg Chl *a*)$^{-1}$ d^{-1}]	14 ± 3	(n=9)	19 ±5	(n=8)
POC:PON [mol mol^{-1}]	6.3 ± 0.6	(n=25)	5.9 ±0.5	(n=24)
POC:Chl *a* [g:g]	0.03 ±0.01	(n=8)	0.04 ±0.02	(n=5)
PAR [mol photons m^{-2} d^{-1}]	13 ± 5	(n=9)	15 ±6	(n=9)
MLD [m]	71 ± 14	(n=10)	35 ±13	(n=10)
NO_3 [mmol m^{-3}]	19.9 ± 0.5	(n=35)	16.3 ±1.8	(n=26)
PO_4 [mmol m^{-3}]	1.3 ± 0.1	(n=35)	1.2 ±0.1	(n=26)
$Si(OH)_4$ [mmol m^{-3}]	4.5 ± 3.1	(n=35)	2.2 ±1.3	(n=26)
NO_3 deficit concentration [mmol m^{-3}]	9.1 ±0.9	(n=35)	10.2 ±2.6	(n=26)
PO_4 deficit concentration [mmol m^{-3}]	0.6 ±0.1	(n=35)	0.6 ±0.2	(n=26)
$Si(OH)_4$ deficit concentration [mmol m^{-3}]	22.6 ±2.5	(n=35)	19.7 ±5.3	(n=26)
NO_3 deficit [mmol m^{-2}]	1087 ±108	(n=35)	1219 ±307	(n=26)
PO_4 deficit [mmol m^{-2}]	75 ± 7	(n=35)	68 ± 18	(n=26)
$Si(OH)_4$ deficit [mmol m^{-2}]	2712 ±303	(n=35)	2359 ± 631	(n=26)
NO_3:PO_4 deficit [mol mol^{-1}]	14.4 ± 0.9	(n=35)	17.9 ± 0.9	(n=26)
$Si(OH)_4$:NO_3 deficit [mol mol^{-1}]	2.5 ± 0.3	(n=35)	2.0 ± 0.4	(n=26)
TDFe [nM]	0.12 ± 0.03	(n=48)	0.14 ± 0.03	(n=11)

Figure 1

Click here to download high resolution image

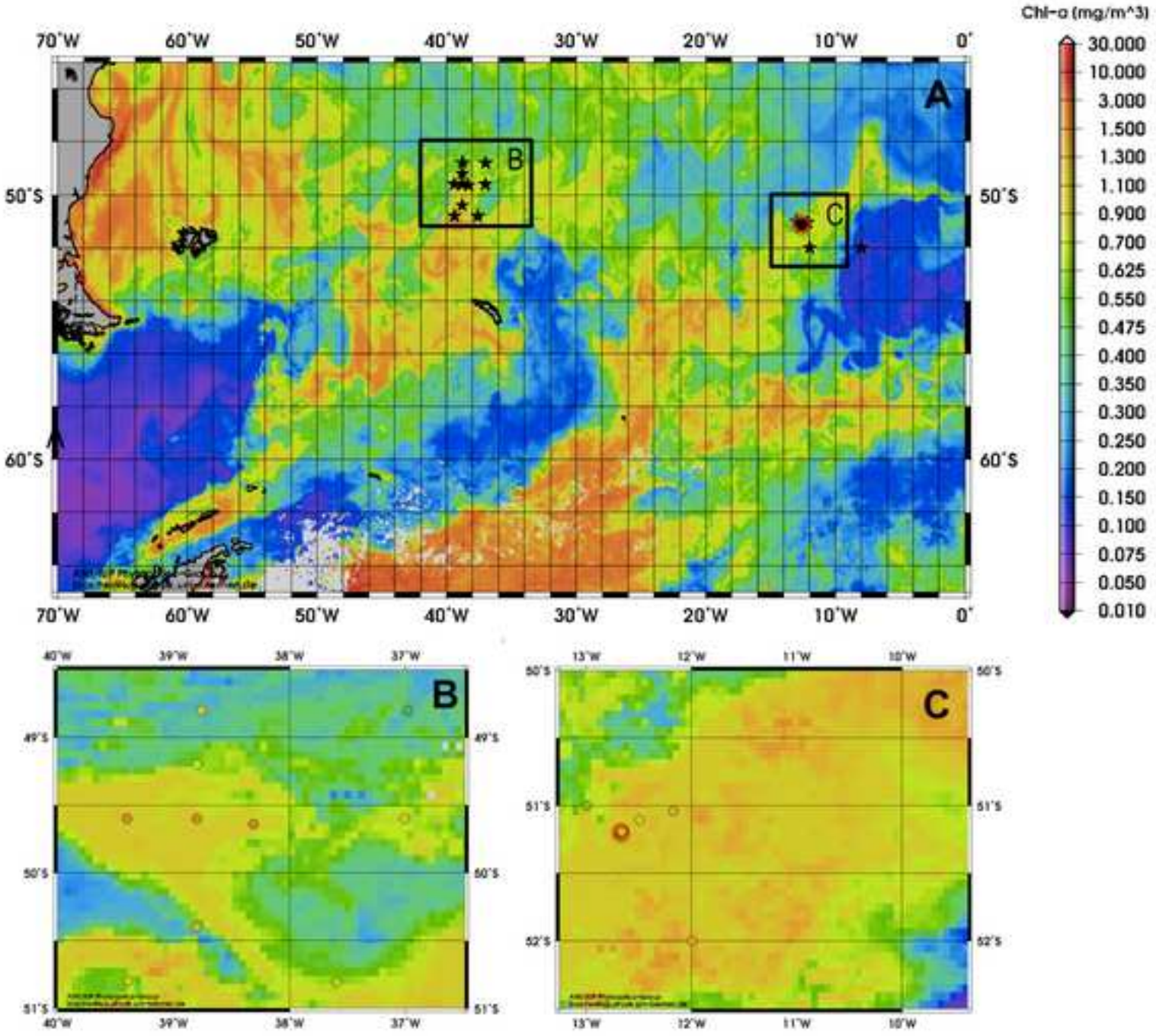

Figure 2

Click here to download high resolution image

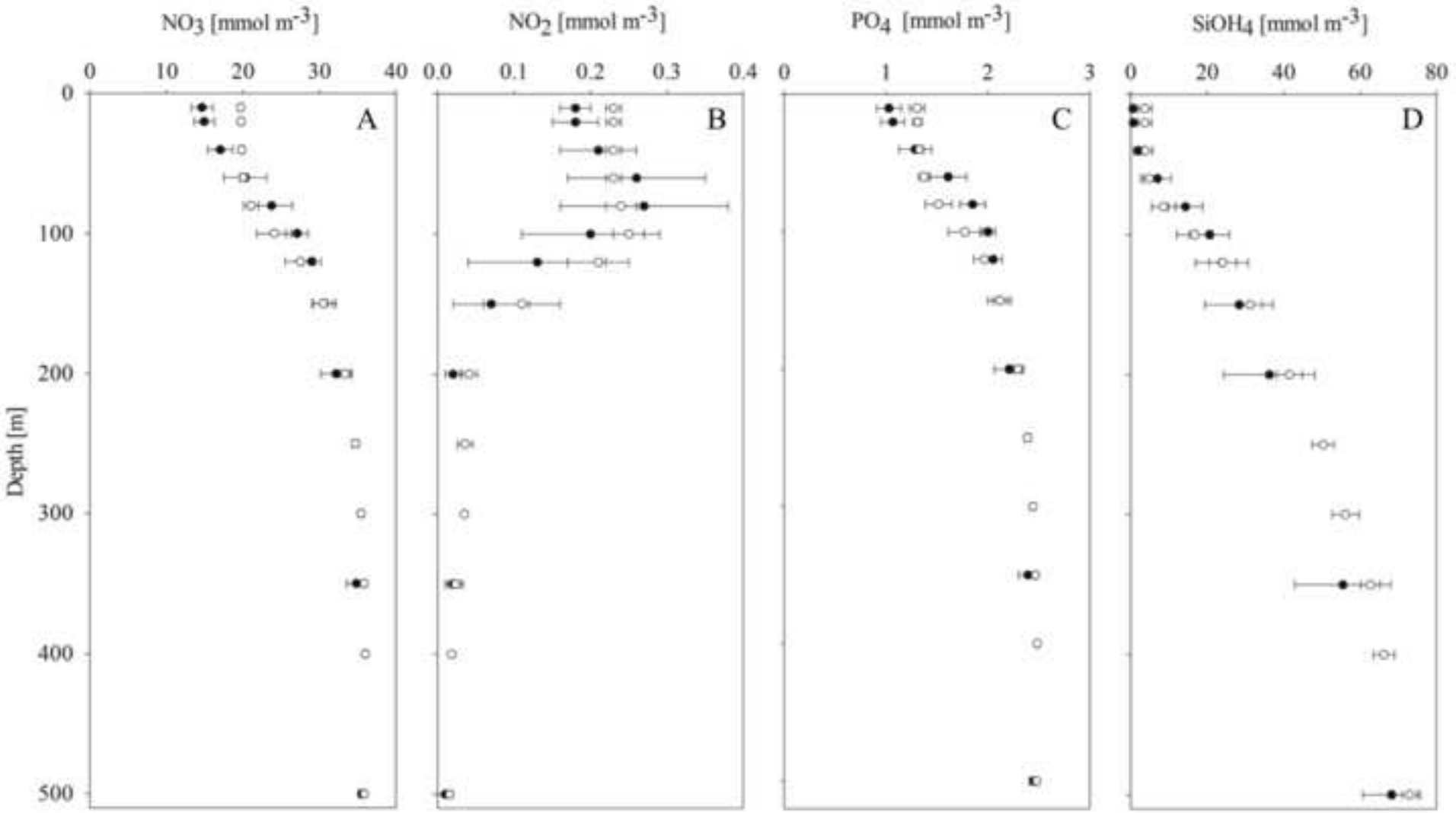

Figure 3

Click here to download high resolution image

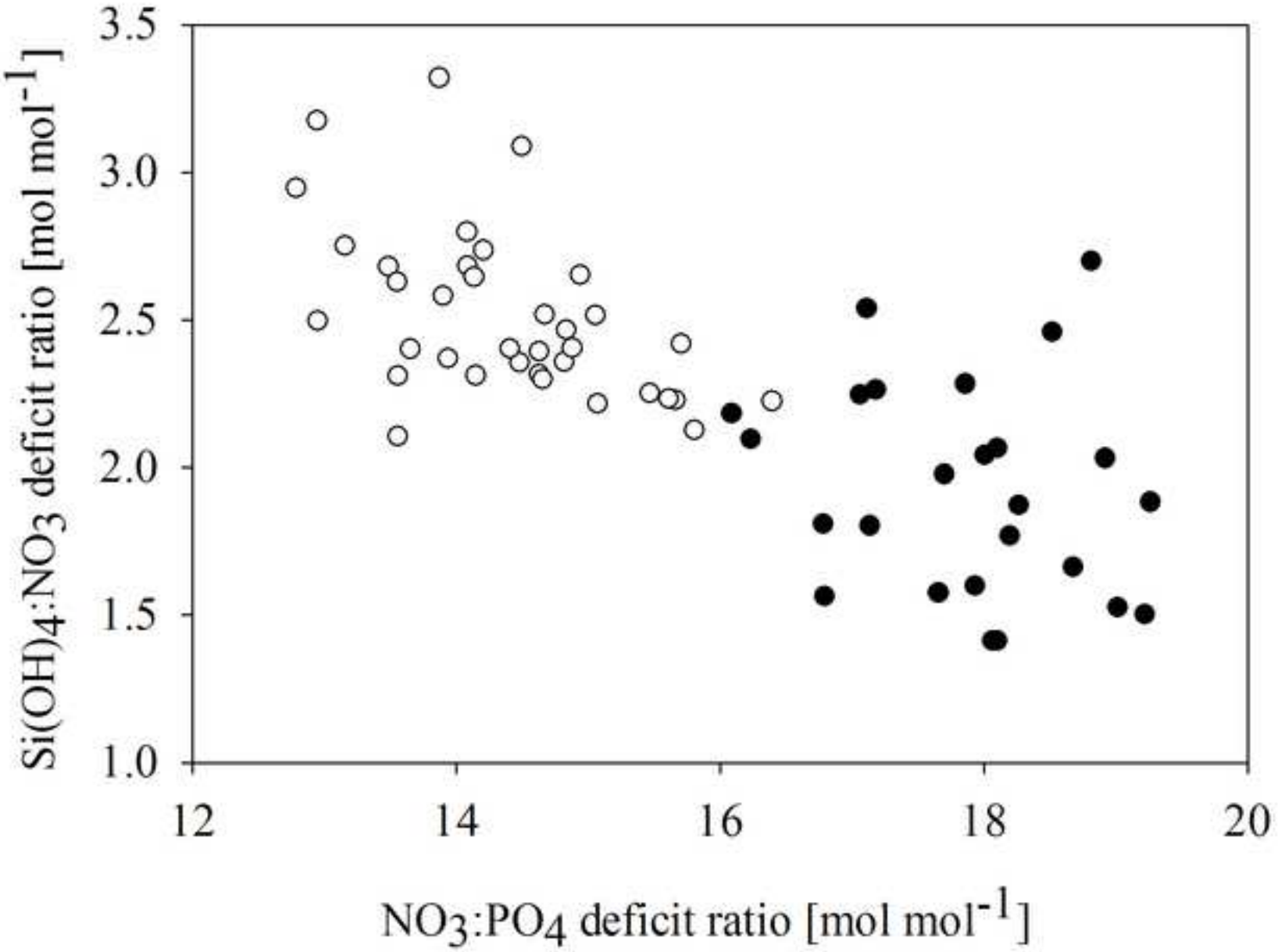

Figure 4

Click here to download high resolution image

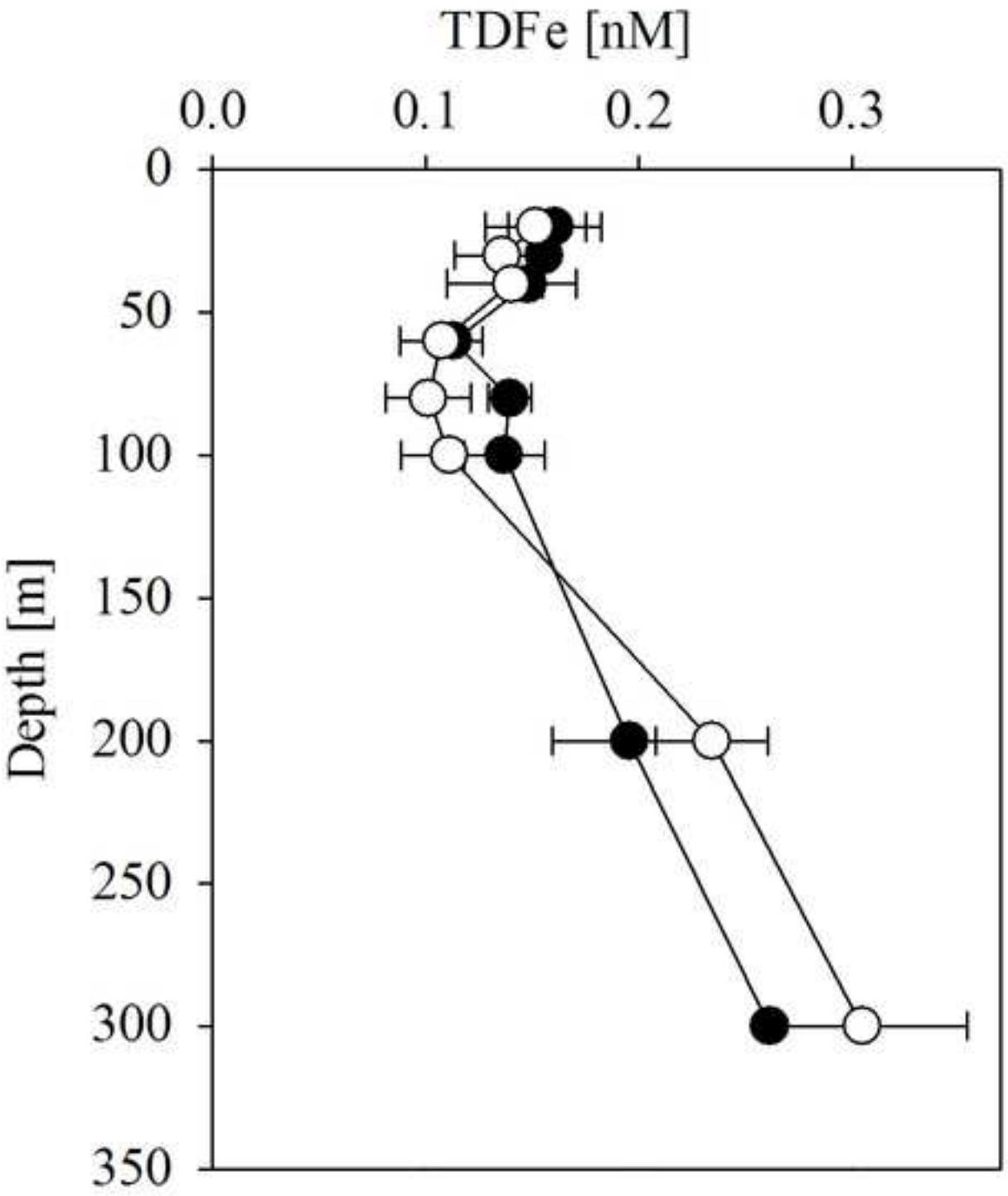

Figure 5

Click here to download high resolution image

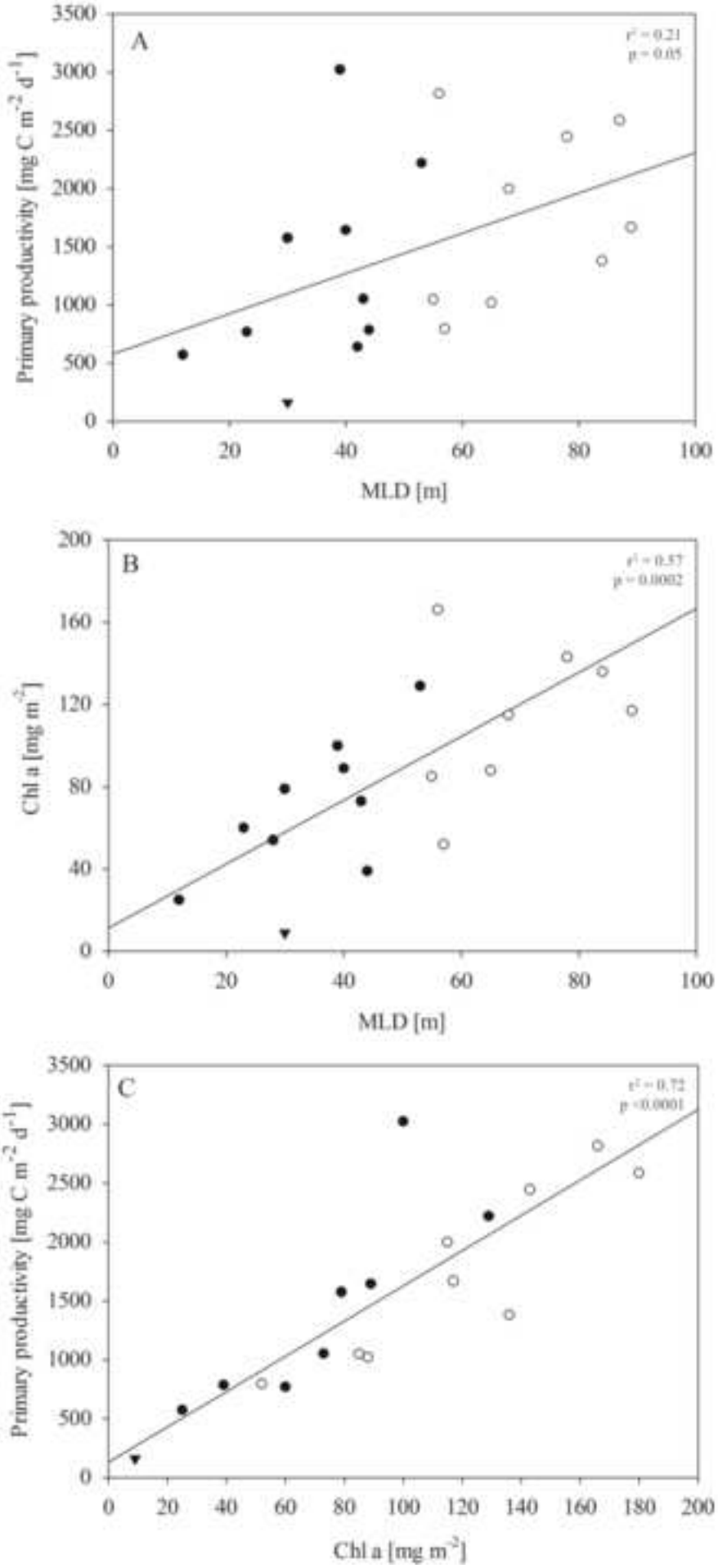

Figure 6

Click here to download high resolution image